GREEN SYNTHESIS OF ZnO & Cu DOPED ZnO NANOPARTICLES USING LEAF EXTRACT OF *Azadirachta indica*: ITS APPLICATION ON THE DRUG RESISTANT BACTERIA

BY

DAWIT TAMIRE

A THESIS SUBMITTED TO THE DEPARTMENT OF CHEMISTRY
SCHOOL OF APPLIED NATURAL SCIENCE
PRESENTED IN PARTIAL FULFILMENT OF THE REQUIREMENT FOR THE DEGREE OF MASTER OF SCIENCE IN CHEMISTRY

OFFICE OF GRADUATE STUDIES
ADAMA SCIENCE AND TECHNOLOGY UNIVERSITY

OCTOBER, 2017
ADAMA, ETHIOPIA

GREEN SYNTHESIS OF ZnO & Cu DOPED ZnO NANOPARTICLES USING LEAF EXTRACT OF *Azadirachta indica*: ITS APPLICATION ON THE DRUG RESISTANT BACTERIA

BY

DAWIT TAMIRE

MAJOR ADVISOR: ENYEW AMARE (PhD)

CO – ADVISOR: BEDASA ABDISA (PhD)

A THESIS SUBMITTED TO THE DEPARTMENT OF CHEMISTRY

SCHOOL OF APPLIED NATURAL SCIENCE

PRESENTED IN PARTIAL FULFILMENT OF THE REQUIREMENT FOR THE DEGREE OF MASTER OF SCIENCE IN CHEMISTRY

OFFICE OF GRADUATE STUDIES

ADAMA SCIENCE AND TECHNOLOGY UNIVERSITY

OCTOBER, 2017

ADAMA, ETHIOPIA

APPROVAL OF BOARD OF EXAMINERS

We, the undersigned, members of the Board of Examiners of the final open defense by Dawit Tamire have read and evaluated his thesis entitled "**GREEN SYNTHESIS OF ZnO & Cu DOPED ZnO NANOPARTICLES USING LEAF EXTRACT OF *Azadirachta indica*: ITS APPLICATION ON THE DRUG RESISTANT BACTERIA**" and examined the candidate. This is, therefore, to certify that the thesis has been accepted in partial fulfillment of the requirement of the Degree of Master of Science in Chemistry.

Enyew Amare (PhD)		02/10/2017
Advisor	Signature	Date
Bedasa Abdisa (PhD)		02/10/2017
Co - Advisor	Signature	Date
Genechu Dereje (PhD)		02/10/17
Chairperson	Signature	Date
Fedlu Kedir (PhD)		30, 09, 2017
Internal Examiner	Signature	Date
Alemayew P. Washe (PhD)		26/09/2017
External Examiner	Signature	Date

DECLARATION

I hereby declare that this M.Sc Thesis is my original work and has not been presented for a degree in any other university, and all sources of material used for this thesis have been duly acknowledged.

Name: Dawit Tamire

Signature:_____

This M.Sc Thesis has been submitted for examination with our approval as thesis advisors.

Advisor Name: Enyew Amare (PhD) Co-advisor Name: Bedasa Abdisa (PhD)

Signature:_____ Signature:_____

Date of submission:_____

ADVISOR'S APPROVAL SHEET

To: Chemistry Department

Subject: Thesis Submission

This is to certify that the thesis entitled "**GREEN SYNTHESIS OF ZnO & Cu DOPED ZnO NANOPARTICLES USING LEAF EXTRACT OF *Azadirachta indica*: ITS APPLICATION ON THE DRUG RESISTANT BACTERIA**" submitted in partial fulfillment of the requirements for the degree of Master of Science in Chemistry, the Graduate program of the department of Chemistry, and has been carried out by Dawit Tamire Id. No GSR/6155/04, under our supervision. Therefore, we recommend that the student has fulfilled the requirements and hence hereby he can submit the thesis to the department.

Name of major Advisor	Signature	Date
Name of Co-Advisor	Signature	Date

DEDICATION

This Thesis manuscript is dedicated to my beloved wife Yehualashet Gebremichael for her concern, love, patience and affection.

ACKNOWLEDGEMENTS

First I would like to thank almighty God who gave me strength and wisdom to complete my work successfully.

Then I would like to express my genuine heartfelt gratitude to my advisor, Dr. Enyew Amare for his invaluable suggestion, comments, corrections, professional & technical guidance and friendly approach throughout my work for the successful accomplishment of this thesis.

I would like to express my deepest gratitude to my Co-adviser Dr. Bedasa Abdisa, for his patience, fruitful advice and friendly approach throughout my work.

I would like to express my thanks to the Program of Applied Chemistry, Adama Science and Technology University, for providing the necessary knowledge, assistance and facilities to conduct my research work. I would like to extend my sincere thanks to Ato Solomon Girmay, head of Applied Chemistry Program in Adama Science and Technology University, for his help and moral support.

I would like to take the opportunity to thank Addis Ababa University, Department of Chemistry for allowing me to use XRD, FT-IR and UV-Visible spectroscopy. My thanks also goes to Professor T. Ganesh for assisting me for SEM and EDX analysis which is done in India.

I also highly acknowledge the generous contribution of Oromiya Public Health Research, Capacity Building and Quality Assurance Laboratory center for their cooperation to perform the antibacterial activity.

My acknowledgement is also extended to Ministry of Education for giving me the opportunity to join this postgraduate program and for sponsorship of my study.

Finally, my cheerful thanks go to my parents and all the family members who give me moral and material support during my study.

TABLE OF CONTENTS

Contents **Page**

DECLARATION……....iv
DEDICATION……....vi
ACKNOWLEDGEMENTS……...vii
LIST OF TABLES…….....xi
LIST OF FIGURES……...xii
LIST OF APPENDICES……..xiv
LIST OF ABBREVIATIONS……...xv
ABSTRACT……xvi
1. INTRODUCTION…….. 1
1.1 Background of the Study..... 1
1.2 Statement of the Problem 3
1.3 Objectives of the Study 4
1.3.1 General Objective 4
1.3.2 Specific Objectives 4
1.4 Significance of the Study 4
1.5 Scope of the Study..... 4
2. LITERATURE REVIEW…… 5
2.1 Synthesis of ZnO Nanoparticles..... 5
2.1.1. Physical Method 5
2.1.2. Chemical Method 6
2.1.3 Biological Method 7
2.2 ZnO Nanoparticles 8
2.3 Properties of Zinc Oxide Nanoparticles 9
2.3.1 Electrical Properties..... 9
2.3.2 Optical Properties 9
2.3.3 Chemical Properties..... 10
2.4 Green Synthesis of Nanoparticles 11
2.5 Antibacterial Activity of ZnO Nanoparticles 11

2.6 Applications of Zinc Oxide Nanoparticles 12
3. MATERIALS AND METHODS……...
Error! Bookmark not defined.
3.1. Materials 13
3.1.1 Chemicals and Solvents 13
3.1.2 Apparatus 13
3.2 Methods 13
3.2.1 Collection of Plant Material 13
3.2.2 Preparation of the Leaf Extract 14
3.2.3 Preparation of Precursors and Synthesis of pure and Cu doped Zinc Oxide Nanoparticles 15
3.2.3.1 Using Zinc Acetate Dihydrate [$Zn(CH_3COO)_2.2H_2O$] 15
3.2.3.2 Using Zinc Nitrate Hexahydrate [$Zn(NO_3)_2.6H_2O$] 16
3.2.3.3 Synthesis of Cu Doped ZnO Nanoparticles 16
3.3 Characterization Methods of Zinc Oxide Nanoparticles 19
3.3.1. Thermal Gravimetric Analysis (TGA) 19
3.3.2. X-Ray Diffraction (XRD) 19
3.3.3. Scanning Electron Microscopy (SEM) 19
3.3.4. Energy Dispersive X- Ray Spectroscopy 20
3.3.5. Fourier Transform Infrared (FT-IR) Spectroscopy 20
3.3.6. UV-Visible Spectroscopy 20
3.4 Method for Antibacterial Activity 20
3.4.1 Preparation of Inoculum 20
3.4.2 Inoculation of Test Plate 21
3.4.3 Disc Diffusion Method for Antibacterial Activity 21
4. RESULTS AND DISCUSSION……23
4.1. Thermal Gravimetric Analysis (TGA) 23
4.2. X-Ray Diffraction (XRD) 24
4.3. Scanning Electron Microscopy (SEM) Analysis 31
4.4. Energy Dispersive X-Ray Spectroscopy (EDX) Analysis 33

4.5. Fourier Transformed Infrared (FT-IR) Spectroscopy Analysis 37
4.6. UV – Visible Spectroscopy Analysis 42
4.7. Antibacterial Activity of ZnO NPs and Cu Doped ZnO NPs 45
5. CONCLUSIONS……..51
REFERENCES…….. 52
APPENDICES……...57

LIST OF TABLES

Table **Page**

Table 1: d- spacing (d_{hkl}) and Miller indices for ZNS1 and ZAS1……...…….27

Table 2: FWHM values, crystallite sizes, d - spacing (d_{hkl}) and Miller indices for ZAS4(1:1)…….29

Table 3: d- spacing (d_{hkl}) and Miller indices for CDS1 and CDS3……29

Table 4: Different angles and their corresponding FWHM values and sizes of ZnO nanoparticles using zinc nitrate and zinc acetate precursors……...30

Table 5: Different angles and their corresponding FWHM values and sizes of Cu doped ZnO nanoparticles using zinc acetate and copper nitrate precursors……...30

Table 6: Quantitative analysis of ZAS1 (9:1)…….....33

Table 7: Quantitative analysis of ZAS2 (7:3)……34

Table 8: Quantitative analysis of ZAS3 (3:2)……35

Table 9: Quantitative analysis of CDS3……..36

Table 10: Inhibition zone (mm) of ZnO nanoparticles and Cu doped ZnO nanoparticles against gram positive and gram negative bacterial strains……46

Table 11: Inhibition zone (mm) size against *Staphylococcus aureus*, *Bacillus subtilis*, and *Escherichia coli* by various antibiotics……49

LIST OF FIGURES

Figures **Page**

Figure 1: Synthesis of nanoparticles by physical (top down) and chemical (bottom up) methods ……7

Figure 2a: Leaves of Neem (*Azadirachta indica*) taken from ASTU……....14

Figure 2b: (A) Leaves of neem (*Azadirachta indica*); (B) planar chemical structure of azadirachtin molecule……14

Figure 3: Thermal Analysis result for uncalcinated ZnO NPs using zinc acetate (UZAS1)…….23

Figure 4: Thermal Analysis result for uncalcinated $Zn_{0.995}Cu_{0.005}$(UCDS1)……24

Figure 5: XRD pattern of ZnO nanoparticles……26

Figure 6: XRD pattern for ZnO nanoparticles synthesized using zinc acetate and Neem leaf extract (1:1).....28

Figure 7: SEM images of ZnO Nanoparticles……....32

Figure 8: EDX Spectrum of ZAS1 (9:1)……33

Figure 9: SEM images of selected area for EDX spectra of ZAS1……...33

Figure 10: EDX Spectrum of ZAS2 (7:3)…….….34

Figure 11: SEM images of selected area for EDX spectra of ZAS2…….34

Figure 12: EDX Spectrum of ZAS3 (3:2)……..35

Figure 13: SEM images of selected area for EDX spectra of ZAS3…….35

Figure 14: EDX Spectrum of CDS3 ($Zn_{0.985}Cu_{0.015}O$) …….36

Figure 15: SEM images of selected area for EDX spectra of CDS3 ($Zn_{0.985}Cu_{0.015}O$)……36

Figure 16: FT-IR spectrum for uncalcinated ZnO nanoparticles synthesized using zinc nitrate precursor.....37

Figure 17: FT-IR spectrum for uncalcinated ZnO nanoparticles synthesized using zinc acetate precursor……38

Figure 18: FT-IR spectrum for calcinated ZnO nanoparticles synthesized using zinc acetate precursor.....39

Figure 19: FT-IR spectrum for uncalcinated Cu doped ZnO Nanoparticles ($Zn_{1-x}Cu_xO$, x=0.015)……..40

Figure 20: FT-IR spectrum for calcinated Cu doped ZnO nanoparticles ($Zn_{1-x}Cu_xO$, x=0.015)……..41

Figure 21: UV-Vis absorbance of uncalcined ZnO NPs synthesized using zinc acetate and Neem leaf extract (9:1)…….42

Figure 22: UV-Vis absorbance of calcined ZnO NPs synthesized using zinc acetate and Neem leaf extract (9:1)…….43

Figure 23: UV-Vis absorbance of uncalcined ZnO NPs synthesized using zinc acetate and Neem leaf extract (7:3)……....43

Figure 24: UV-Vis absorbance of calcined ZnO NPs synthesized using zinc acetate and Neem leaf extract (7:3)…….44

Figure 25: UV-Vis absorbance of calcined ZnO NPs synthesized using Cu doped ZnO NPs ($Zn_{0.985}Cu_{0.015}O$)……45

Figure 26: Zone of inhibition of ZnO nanoparticles against(a) *Staphylococcus aureus*, (b) *Bacillus subtilis*, (c) *Escherichia coli* and (d) *Proteus mirabilis*……...50

LIST OF APPENDICES

Appendix **Page**

Appendix 1: XRD pattern for ZnO NPs using zinc nitrate precursor……57
Appendix 2: XRD pattern for ZnO NPs using zinc acetate precursor……..…….58
Appendix 3: XRD pattern for Cu doped ZnO NPs ($Zn_{0.995}Cu_{0.005}O$)……59
Appendix 4: XRD pattern for Cu doped ZnO NPs ($Zn_{0.985}Cu_{0.015}O$)…….....60

LIST OF ABBREVIATIONS

ZnO	Zinc Oxide
ZnO NPs	Zinc Oxide Nanoparticles
IR	Infrared
UV	Ultraviolet
UV – Vis	Ultraviolet Visible Spectrophotometer
SEM	Scanning Electron Microscope
EDX	Energy Dispersive X-ray spectroscopy
XRD	X – Ray Diffraction
FTIR	Fourier Transform Infrared Spectroscopy
E.Coli	*Escherichia Coli*
S.aureus	*Staphylococcus aureus*
FDA	Food and Drug Administration
USA	United States of America
CaO	Calcium Oxide
MgO	Magnesium Oxide
Cu	Copper
H_2O_2	Hydrogen Peroxide
DNA	Deoxyribonucleic Acid
ROS	Reactive Oxygen Species
DMF	N, N – Dimethyl Formamide
PVP	Poly N – Vinyl Pyrrolidine
CTAB	Cetyl trimethyl Ammonium Bromide
eV	Electron Volt
meV	mili electron Volt
LED	Light Emitting Diodes
$Zn_{1-x}Cu_xO$	Copper doped zinc oxide(x=0.005, 0.01 & 0.015)
TGA	Thermal Gravimetric Analysis

DTA Differential Thermal Analysis

rpm revolution per minute

ABSTRACT

The progress of green chemistry in the synthesis of nanoparticles using plants has attracted a great attention due to its low cost and non-toxic and environment-friendly nature. The present study focuses on the biological synthesis and characterization of pure and Cu-doped zinc oxide nanoparticles using different ratios of neem leaf extract and the nanoparticles for antibacterial application on the drug resistant bacteria. Zinc Nitrate hexahydrate and zinc acetate dihydrate were used as precursor to synthesize ZnO nanoparticles whereas zinc acetate dihydrate and copper nitrate trihydrate were used to synthesize Cu-doped ZnO nanoparticles. The synthesized nanoparticles were characterized by advanced techniques like Thermo Gravimetric Analysis (TGA), X-Ray Diffraction (XRD), Scanning Electron Microscopy (SEM), Energy Dispersive X-Ray Spectroscopy (EDX), Fourier Transform Infrared Spectroscopy (FT-IR), and UV-Visible spectroscopy. TGA was performed to study the thermal stability of pure & Cu doped ZnO nanoparticles and the results showed that the synthesized materials were stable above 400°C. The desired phase formation and crystal structure of the synthesized materials were followed by X – Ray Diffraction (XRD) analysis. The XRD analysis revealed that all the synthesized particles have pure hexagonal phase with particle size in the range of 16 – 24 nm. The SEM analysis indicated the spherical shape morphology for the samples that were calcinated at 400 ^{0}C and their grain size increased with the decrease of the concentration of the capping agents or leave extract. EDX spectra showed the elemental composition of the synthesized nanoparticles. The FT-IR technique has been used to study the interaction between the capping agents and the synthesized ZnO nanoparticle which was also confirmed by SEM studies. The UV-Visible investigation also confirmed the formation nanoparticle, the absorbance peak at 376 nm corresponding to the characteristic band of zinc oxide nanoparticles. The antibacterial activity studies of the synthesized materials against *Staphylococcus aureus*, *Bacillus subtilis*, *Escherichia coli*, and *Proteus mirabilis* have better performance with the reference to the selected standards gentamicin and ciprofloxacin.

Keywords: *Azadirachta indica*, Zinc oxide nanoparticle, characterization, *Escherichia coli*, Gentamicin

1. INTRODUCTION

1.1 Background of the Study

Nanotechnology is an emerging and a rapidly growing field with its wide application in science and technology for the purpose of manufacturing new material at the nanoscale level (Wildenberg, 2005). It involves the synthesis, characterization and application of nanomaterials by controlling shape and size.

In the field of nanotechnology, the importance of metal oxide nanoparticles is increasing due to their unique optical, catalytic, electronic, magnetic and antimicrobial properties (Gratzel, 2001; Okuda M, 2005; Dai J, 2002). Zinc oxide nanoparticle is one of the important oxides, because of its physical and chemical properties such as stability, photocatalytic activity, luminous transmittance, effective antibacterial property, intensive IR and UV absorption (Murray, 2001; Bhattacharya R, 2008).

Toxicity studies have shown that zinc ions do not cause any damage to the DNA of human cells (Yamada, 2007, Bhumkar DR J.H., 2007; Sun Y, 2002). This aspect necessitated their usage as antibacterial agents, noxious to microorganisms and hold good biocompatibility to human cells. ZnO nanoparticles have the tremendous applications as antimicrobial agents and possess strong antibacterial activity against high temperature and pressure resistant spores. It is believed that the antimicrobial activity of the ZnO nanoparticles might be either due to the generation of hydrogen peroxide or due to the electrostatic binding of the particles on the microbial surface (Yin B, 2003).

Synthesis of nanoparticles can be performed using a number of routinely used chemical methods such as chemical precipitation, sonochemical, solvothermal, sol-gel process, hydrothermal decomposition etc (Callegari A, 2003; Dimitrijevic NM, 2001, Zhang L, 2006). Chemical methods are popular for the synthesis but the uses of toxic chemicals and the cost limits their application. An eco friendly green mediated synthesis of inorganic nanoparticle is a fast growing research area (Sathya, 2012; Nagajyoti, 2011).

Recently biological methods for synthesis of zinc oxide nanoparticle using microorganisms, enzymes, and plant extracts have been suggested as possible eco-friendly alternatives to chemical and physical methods (Awwad, 2014). Plant extract as bio-templates can be an economic and efficient alternative for the large scale synthesis of nanoparticles. Green synthesis of nanoparticles with plant leaf extract, an innovative branch of nanotechnology, has gained significant importance in recent years and has become one of the most preferred methods (Ashe, 2011, Senthilkumar, 2014).

Azadirachta indica commonly known as Neem belongs to *Meliaceae* family (Monica, 2013). Every part of the tree has been used as a traditional medicine for household remedy against various human ailments, from antiquity. Neem leaf extract has also been used for the synthesis of silver and gold. The major advantages of using Neem leaves extract for the present study include;

(i) Neem is a quite commonly available medicinal plant and abundant in nature;

(ii) The synthesis method excludes addition of external stabilizing agent during synthesis; and

(iii) It offers synergistic effects to enhance the antimicrobial properties of the synthesized ZnO nanoparticles (Asmita J.Gavhane, 2012).

The antimicrobial activity of zinc oxide nanoparticles is well known and hence we made use of this property to inhibit growth of two gram positive bacteria (*Staphylococcus aureus* and *Bacillus subtilis)* and two gram negative bacteria *(Escherichia coli* and *Proteus mirabilis*) using disc diffusion method. These four bacterial strains were selected as they are highly contagious. Hence, the potential antimicrobial activities of zinc oxide nanoparticles against these pathogenic bacteria were evaluated in this work. These four different types of pathogenic bacteria have been chosen for the study because of the following reasons:

Staphylococcus aureus is a gram-positive, round-shaped bacterium that is a member of the Firmicutes, and is frequently found in the nose, respiratory tract, and on the skin (Firouzabadi, 2015). ***Bacillus subtilis*** is gram-positive coccoid bacterium causes pneumonia, meningitis, sepsis (Haritha Meruvu, 2011). ***E. coli*** is gram-negative bacteria, virulent strain causes food poisoning, urinary tract infection, neonatal meningitis (Haritha Meruvu, 2011). ***Proteus mirabilis*** is a gram-

negative, facultative anaerobic, rod-shaped bacterium that is frequently isolated from clinical specimens. Its most common site of infection is the urinary tract (Slman, 2012). The present study describes the synthesis of pure and doped ZnO nanoparticles by biological method from the leaf extract of Neem (*Azadirachta indica*), characterization and its applications in antibacterial activity.

1.2 Statement of the Problem

During the last decade, a rapidly increment in the development of new antibacterial materials has been observed as consequence to the spread of antibiotic resistant infections, which has become a major issue in health care. The emerging infectious diseases and the development of drug resistance bacteria at an alarming rate is a matter of serious concern and increasing public health problem. New strategies for controlling bacterial activity are urgently needed and nanomaterials can be a very promising approach. A possible alternative is the synthesis of new inorganic compounds with antimicrobial properties. Zinc oxide nanoparticle has the advantage of durability as well as chemical and physical stability over common organics and antibiotics compounds. Many research works had been concerned with green synthesis of nanoparticles for the antibacterial applications which is the recent research focus. However, few studies have been conducted to evaluate the antibacterial effects of zinc oxide nanoparticles on gram positive and gram negative bacteria. Moreover, the antibacterial mechanism of zinc oxide nanoparticles is still unclear. Therefore, this study was undertaken to investigate the antibacterial activity against gram positive and gram negative bacterial strains using disc diffusion method. Hence this research is intended to fill the gap in the area of green synthesis of ZnO nanoparticles from the leaves of *Azadirachta indica* and its application for drug resistant bacteria. Therefore, the work is planned to synthesize pure and Cu - doped zinc oxide nanoparticles using neem leaf extract and investigate the effect of pure and doped ZnO nanoparticle against gram positive bacteria (*Staphylococcus aureus* and *Bacillus subtilis)* and gram negative bacteria (*Escherichia coli* and *Proteus mirabilis*).

1.3 Objectives of the Study

1.3.1 General Objective

The general objective of this study is green synthesis of ZnO and Cu doped ZnO nanoparticles using aqueous extract of *Azadirachta indica* leaves and to study their antibacterial activity against drug resistant bacteria.

1.3.2 Specific Objectives

The specific objectives of this work are to

- Synthesize ZnO and Cu doped ZnO nanoparticles using aqueous extract of neem leaves, *Azadirachta indica.*
- Characterize the synthesized ZnO and Cu doped ZnO nanoparticles using XRD, SEM, EDX, FT-IR and UV- Visible.
- Investigate the effect of pure and Cu doped ZnO nanoparticles against *Staphylococcus aureus, Bacillus subtilis, Escherichia coli and Proteus mirabilis* bacteria.

1.4 Significance of the Study

This study will provide important information about the green synthesis strategy of ZnO and Cu doped ZnO nanoparticles and their antibacterial activity.

1.5 Scope of the Study

The scope of the study is limited to green synthesis of pure and Cu-doped ZnO nanoparticles at low concentration of Cu ion using neem leaf extract and characterization of the synthesized NPs using UV-Vis, XRD, FT-IR, SEM, EDX and TGA techniques, and investigation of antibacterial activity of the NPs against four bacteria: *Staphylococcus aureus, Bacillus subtilis, Escherichia coli* and *Proteus mirabilis.*

2. LITERATURE REVIEW

2.1 Synthesis of ZnO Nanoparticles

Synthesis of dimensionally controlled particles in large quantities and study of their properties to investigate novel applications is a preferred activity for researchers in nanomaterials. There are several physical and chemical procedures for synthesis of ZnO nanoparticles in large quantities in a short period of time. Among them simple-solution based methods, chemical precipitation, sol-gel, solvothermal or hydrothermal, electrochemical, and photochemical reduction method are preferable methods. ZnO nanoparticles can be synthesized form various species of plant leaf extract, microorganisms like bacteria, and fungi cellular extract using green synthesis methods. The green synthesis of nanoparticles also governs by various enzymes. There are different methods of ZnO nanostructures preparation like metal organic vapour phase epitaxy, evaporation of high temperature, gas spraying, pulsed laser deposition, sputtering, sol-gel, wet chemical and electrochemical methods. Different applications of nanoparticles based on different protocols which have been designed for synthesis of nanoparticles (Wang, 1999).

2.1.1. Physical Method

Physical methods developed for synthesis of ZnO nanoparticles often require special equipments or operational control. The physical method often called top-down approach which includes methods like diffusion, irradiation, thermal decomposition, and arc discharge. The thermal decomposition method is one of the significant top-down approaches. It is used for the creation of monodisperse nanoparticles. These approaches use larger initial structures or macroscopic units which can be externally controlled in the processing of nanostructures. Etching through the mask; ball milling and application of severe plastic deformation are common examples of physical top-down method of synthesis of nanoparticles. The top-down method of synthesis is a model which generates on a larger scale for further reduction of nano scale. Mostly the top-down methods are not cheap and quick to manufacture. This method is slow and not suitable for large scale production (Reddy, 2006).

In this method of synthesis fatty acids are allowed to dissolve in the hot NaOH solution and then mixed with the metal salt solution. After that, the solution used to form the metal precipitates.

Crystals and short wires of copper are allowed to be encircled in the glass ampoules by the diffusion method. Then, it is sealed at low pressure followed by annealing at 500 ^{0}C for 24 hours. Subsequently the crystals are eradicated from the ampoules. At room temperature, the ampoules free crystals are chilled on a metallic plate. In UV irradiation method, polycarbonate films are placed on glass microscope slide .Then this slide is exposed to UV radiation (Wang,1999).

2.1.2. Chemical Method

Moderate reaction conditions and convenient synthetic manipulation have rendered chemical methods an attractive option for accessing ZnO nanoparticles. Traditional chemical routes that are frequently used in recent years include sol-gel approach, chemical precipitation and colloidal synthesis. Surfactants or polymer based preparative method for ZnO nanomaterials are also quite popular to avoid agglomeration and achieve better control of ZnO nanoparticles. Removal of surfactants or polymers, however, poses serious limitations to such methods. Hence, delicate and precise control of experimental factors for the synthesis of nanoparticles with desired morphologies is a cherished goal for future device applications. Homogeneous chemical precipitation method is often considered economically viable for preparation of monodisperse metal oxide particles of different shapes and sizes. The method also provides better control of chemical and morphological characteristics (Bhattacharjee, 2011).

Chemical methods, including precipitation from inorganic or organic solutions and sol-gel techniques can conveniently provide control of nucleation, growth and ageing of particles in the solution. The methods rely on advanced solution and coordination chemistry theories, enabling the synthesis of the required precursor particles utilizing a variety of parameters to enable control of the solid formation process. A major contribution to the growth of particles is through Ostwald ripening, where small particles with lower solubility product dissolve and re-precipitate on the surface of larger particles in solution. Agglomeration takes place in solution as the particles clog together to minimize surface energy (Z.L. Wang, 2004).

Mostly the chemical methods of synthesis of nanoparticles are the bottom up approaches. These approaches include the miniaturization of material components (up to atomic level) with further

self-assembly processes leading to the formation of nanostructures. During self-assembly the physical forces operating at nano scale are used to combine basic units into larger stable structures. Typical examples are quantum dot formation during epitaxial growth and formation of nanoparticles from colloidal dispersion. In these methods different metal particles are reduced to form nanoparticles. Various types of metal particles used like Sodium borohydrate and Sodium citrate etc. (Jana, 2000). Other chemical reagents used are N, N-dimethylformamide (DMF), Poly (N-vinyl pyrrolidine (PVP), ethyl alcohol, Cetyl trimethyl ammonium bromide (CTAB), etc. (Rai, 2008). This method initiates with a pattern which is generate larger scale, then reduced to nano scale. This method of synthesis of nanoparticles is cheap and quick to manufacture. However, it is not suitable for the large scale production.

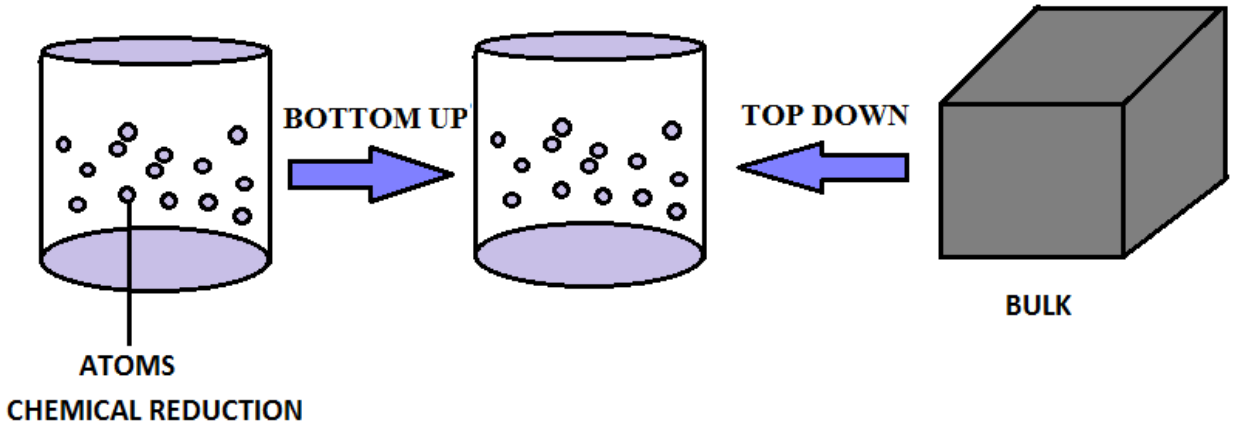

Figure 1: Synthesis of nanoparticles by physical (top down) and chemical(bottom up) methods

2.1.3 Biological Method

Green synthesis method is proved as beneficial over other methods which are implemented for the synthesis of nanoparticles. Green synthesis methods are eco-friendly approach and compatible for pharmaceutical and other biomedical applications, as the toxic chemicals are not used in these methods. Besides, this method does not require high pressure, temperature. Synthesis of various nanoparticles by microorganisms is used more than the other techniques due to its ecofriendly nature. The use of environmentally beneficial materials like plant leaf extract, bacteria, fungi and enzymes for the synthesis of zinc nanoparticles proposes abundant benefits of

ecofriendliness and compatibility for pharmaceutical and many other biomedical applications (Willner B., 2007).

2.2 ZnO Nanoparticles

Zinc oxide (ZnO) is a class of inorganic metal oxides available and exhibits a wide range of nanostructures. Photocatalytic and photooxidizing ability against chemical and biological species are used to characterize these metal oxides. U.S. Food and Drug Administration have recognized ZnO is considered "generally recognized as safe" (GRAS) (M. Premanathan, 2011). Lower cost, UV blocking properties, high catalytic activity, large surface area, white appearance and their remarkable applications in the field of medicine and agriculture are the advantages of ZnO particles. Recently, ZnO have been used extensively in environmental remediation and antibacterial activity (S. Kuriakose, 2013).

ZnO nanoparticles exhibit strong antibacterial activity against high temperature and pressure resistant spores. It is postulated that the generation of hydrogen peroxide or due to the electrostatic binding of the particles on the microbial surface contribute to the antimicrobial activity of ZnO nanoparticles (L. Zhang, 2007). Antibacterial activity of ZnO nanoparticles is of remarkable applications in designing microbial resistant articles for preserving food and wood products, cosmetics, novel nanomedicines wound dressing and disinfecting agents. Photocatalytic activity of ZnO nanoparticles offers a promising method for waste water treatment (B. Srinivasa. Reddy, 2012). Toxic water pollutants released from textile and dying industries by utilizing natural source of energy, sunlight are degraded by ZnO and exhibit photochemical reactivity. This could be because of the presence of many active sites and fabrication of hydroxyl radicals on ZnO surface (S. Baruah, 2009).

Zinc oxide has vast applications in optical, piezo electric, magnetic, and gas sensing. They exhibits high catalytic efficiency, strong adsorption ability and used in sunscreens manufacture, ceramics and rubber processing, waste water treatment, and fungicide. ZnO nanoparticles can absorb UV radiation and therefore offers better protection and improved opaqueness (Theodore, 2006).

2.3 Properties of Zinc Oxide Nanoparticles

The semiconductors with the dimensions in the nanometer are important because of their electrical, optical and chemical properties which can be tuned by the changing the size of particles.

2.3.1 Electrical Properties

The fundamental study of the electrical properties of ZnO nanostructures is crucial for developing their future applications in nanoelectronics. ZnO has a moderately large band gap of 3.3 eV at room temperature. The benefits of a large band gap comprise higher values of breakdown voltages, sustaining large electric fields, high-temperature and high-power operations. ZnO has n-type character, in the absence of doping. The origin of n-type character is typically the non-stoichiometry analysis. Due to the imperfections like the oxygen vacancies, zinc interstitials and ZnO nanowires are reportedly show n-type semiconductor behavior. The major hindrance of ZnO is the broad series of applications in electronics and photonics with the complexity of p-type doping. The favorable and advantageous p-type doping for ZnO nanostructures will enormously enhance their upcoming advance applications in nano scale electronics and optoelectronics. The p-type and n-type ZnO nanowires can serve as p-n junction diodes and the light emitting diodes (LED) (Z.Y.Fan, 2005).

2.3.2 Optical Properties

Zinc oxide is generally transparent to visible light but strongly absorbs ultra violet light below 365.5 nm. The absorption is typically stronger than other white pigments. In the region of visible wavelengths, regular zinc oxide appears white, but, rutile and anatase titanium dioxide have a higher reactive index and thus has a superior opacity. ZnO is a wide band gap of 3.4 eV semiconductor with a large exciton binding energy of 60 meV and also considered as one of the most promising semiconductor material for electronic, photonic, optical and biological applications (Ramani, 2012). The band gap energy occurs between the valence and conducting bands corresponds to the energy of 3655 photons. Zinc oxide is considered as the photoconductive under the analytical study of ultra violet light. The arrangement of optical and semiconductor properties construct a doped zinc oxide which is a contendor for new generations

of devices. Solar cells require Intrinsic optical properties of ZnO nanostructures are being intensively deliberated for the implementing photonic devices. Photoluminescence (PL) spectra of ZnO nanostructures have been extensively reported. Excitonic emissions have been examined from the photoluminescence spectra of the ZnO nanorods. It is shown that quantum size confinement can significantly enhance the exciton binding energy. Strong emission peak at 380 nm due to band-to-band transition and green-yellow emission band related to oxygen vacancy are observed. Photoluminescence spectra show that the ZnO nanowire is a capable and promising material for the UV emission. Its UV lasing property is additionally more significant and interesting. Due to its near-cylindrical geometry and large refractive index of nearly about 2.0, ZnO nanowire or nanorod is a natural candidate for the optical waveguide. The additional advantages of ZnO nanowire lasers are that the excitonic recombination lowers the threshold of lasing, and quantum confinement yields a substantial density of the band edges and enhances radiative efficiency. Optical wave guiding using dielectric nanowire also achieved considerable progress. In recent times, ZnO nanowires were stated as sub-wavelength optical waveguide. Optically forced light emission was guided by ZnO nanowire and coupled into SnO_2 nanoribbon. These discoveries show that the ZnO nanostructures can be potential building blocks for integrated optoelectronic circuits. Optical properties have a great interest towards the vast application of optoelectronics, photovoltaics and biological sensing (Aneesh, 2007).

2.3.3 Chemical Properties

Zinc oxide occurs as the mineral zincite or as white powder known as zinc white. It is usually orange or red in color due to manganese impurity. Crystalline zinc oxide is thermochromic in nature which changes from white to yellow colour when heated and turns back to white colour on cooling. This change in colour is caused by a very small loss of oxygen at high temperatures. Zinc oxide is amphoteric in nature which reacts with both the acids and alkalis. When ZnO reacts with acid, it forms zinc sulfate. Similarly when it reacts with alkali, it forms zincates. ZnO decomposes to form zinc vapor and oxygen indicating its considerable stability. Heating of ZnO with carbon converts the ZnO into Zn which is more volatile in nature. Exposure of zinc oxide to air absorbs both water vapor and carbon dioxide and forms zinc carbonate (J Yu, 2011).

2.4 Green Synthesis of Nanoparticles

Lot of attention has been diverted to the green synthesis of metal nanoparticles using biological material as the reducing and stabilizing agents and due to the usage of eco-friendly, non-toxic and safe reagents during the biosynthesis process, green synthesis has been considered in the field of toxic chemical and physical methods (M. Moritz, 2013). In the biological method, plant extracts are used for controlled and precise synthesis of several metallic nanoparticles. High surface and a large fraction of surface atoms are responsible for the nanoparticles' atom-like behavior (Dijiken A. V., 2000). Despite the fact that conventional methods use less time for synthesizing nanoparticles, they contribute to environmental toxicity because they require toxic chemicals as capping agents. Green nanotechnology is an eco-friendly alternative and is cost effective (S.P. Chandran, 2000) and utilizes proteins as natural capping agents. Synthesis of metal nanoparticles by plants utilizes various secondary metabolites, enzymes, proteins and or other reducing agents.

2.5 Antibacterial Activity of ZnO Nanoparticles

Understanding the mechanism of antibacterial effect of ZnO nanoparticles is necessary to make better use of these nanoparticles in food products and to develop nontoxic, antimicrobial derivatives but the mechanism is not very clear till to date. Some studies have showed that morphology and oxidative stress are responsible for the antibacterial activity of zinc oxide nanoparticles. However, a few studies have suggested that the antibacterial activity might be because of the disruption of cell membrane activity (Brayner, 2006).

Another mechanism might be because of the induction of intercellular reactive oxygen species, including hydrogen peroxide (H_2O_2), which is harmful to bacterial cells. ZnO have also been reported to be activated by UV and visible light in order to generate highly reactive oxygen species such as OH^-, H_2O_2, and O_2^{2-}. These radicals and superoxides cannot penetrate into the cell membrane and are likely to remain on the cell surface, but H_2O_2 penetrate into bacterial cells (Padmavathy, 2008).

The presence of reactive oxygen species (ROS) generated by ZnO nanoparticles was responsible for their bactericidal activity (Yamamoto, 2000). Furthermore, chemical interactions between hydrogen peroxide and membrane proteins, or between other chemical species produced in the

presence of ZnO nanoparticles and the outer lipid bilayer of bacteria could be responsible for the antibacterial behavior of ZnO nanoparticles. The hydrogen peroxide which is produced enters the cell membrane of bacteria and kills them. The study also showed that bacterial growth is inhibited by nano-sized ZnO particles (H. Zhang, 2010). Other study also proposed that the bactericidal activity of ZnO nanoparticles was because of hydrogen peroxide generated by ZnO nanoparticles and the nanoparticles remain in contact with the dead bacteria thereby preventing further bacterial action and continue to generate and discharge hydrogen peroxide to the medium (Padmavathy, 2008).

Phototoxic effect is induced in the aqueous solution of ZnO nanoparticles under UV radiation and produce Reactive Oxygen Species such as hydrogen peroxide (H_2O_2) and superoxide ions (O^{2-}) (H. Zhang, 2011). The active species penetrate into the cells and inhibit or kill microorganisms. This is used in bionanotechnology and in bionanomedicine for many antibacterial applications. Therefore, as ZnO absorbs UV light, enhancement of ZnO bioactivity is thought to be as a result of the produced free radicals (J.T. Seil, 2009).

Among metal oxide powders, ZnO demonstrates very significant growth inhibition of a broad spectrum of bacteria. The suggested mechanism for the antibacterial activity of ZnO is based mainly on the catalysis of formation of the reactive oxygen species (ROS) from water and oxygen that disrupt the integrity of the bacterial membrane although additional mechanisms have also been suggested. Since the catalysis of radical formation occurs on the particle surface, particles with larger surface area demonstrate stronger antibacterial activity. Antibacterial activity of ZnO nanoparticles decreases as the size of the nanoparticles increases (Chehrazi, 2011).

2.6 Applications of Zinc Oxide Nanoparticles

ZnO nanoparticle is used in paints, cosmetics, sunscreens, plastic and rubber manufacturing, electronics and pharmaceuticals products etc. It is also potentially used to treat leukemia and carcinoma cancer cell. It is also a strong antibacterial agent and used as drug carrier. ZnO nanoparticles is also used in industrial sectors including environmental, synthetic textiles, food, packaging, medical care, healthcare, as well as construction and decoration (A. Becheri, 2008).

3. MATERIALS AND METHODS

This chapter presents materials and methods used to carry out the research work. The first section of this chapter describes chemicals and solvents used and the second section presents apparatuses used to carry out the research work. The third section describes methods of synthesizing zinc oxide nanoparticles from different zinc salt precursors using neem leaf extract and the fourth section describes characterization techniques of the synthesized zinc oxide nanoparticles. The fifth and last section describes antibacterial activity of the green synthesized ZnO and Cu doped ZnO nanoparticles.

3.1. Materials

3.1.1 Chemicals and Solvents

The following chemicals and solvents were used in this research work. Zinc nitrate hexahydrate ($Zn(NO_3)_2.6H_2O$, MW = 297.49 (Made in China)), Zinc acetate dihydrate ($Zn(CH_3COO)_2.2H_2O$, MW = 219.5 (Made in China)), Copper(II) nitrate trihydrate ($Cu(NO_3)_2.3H_2O$, MW = 241.63 (UNI-CHEM Chemical Reagents)), Sodium hydroxide (NaOH,M.W = 39.99971g/mol (Ranchem Industry & Trading)), Ethanol absolute(99.9%) (Ranchem Industry & Trading) and deionized water (Ranchem Industry & Trading) were purchased. All chemicals were analytical grade and used without further purification.

3.1.2 Apparatus

The laboratory apparatus used for this work are the following: Whatman filter paper No 1, analytical balance with accuracy of 0.0001g, Magnetic stirrer with hot plate, drying oven and Muffle furnace.

3.2 Methods

3.2.1 Collection of Plant Material

Selection of Plant: The young, disease free and healthy Neem (*Azadirachta indica*) leaves were collected from Adama Science and Technology University campus after conducting the field surveys. The leaves were thoroughly washed and rinsed with deionized water. Then the surface water was dried and the leaf parts weighed about 25 gm.

Figure 2a: Pictures of leaves of Neem (*Azadirachta indica)* taken from ASTU (By Dawit Tamire)

3.2.2 Preparation of the Leaf Extract

The plant leaves were thoroughly washed in deionized water and chopped into small pieces. The aqueous extracts of sample were prepared by boiling the freshly collected cut leaves (25 g) with 100 mL of deionized water at 60 ^{0}C for about 20 minutes using hot plate with magnetic stirrer until the color of the aqueous solution changes from watery to light brown. Then, the extract was cooled to room temperature and filtered using Whatman filter paper No 1. The extract was stored in a refrigerator at 4 ^{0}C in order to be used for further experiments (Manokari M, 2016; Snehal Yedurkar, 2016).

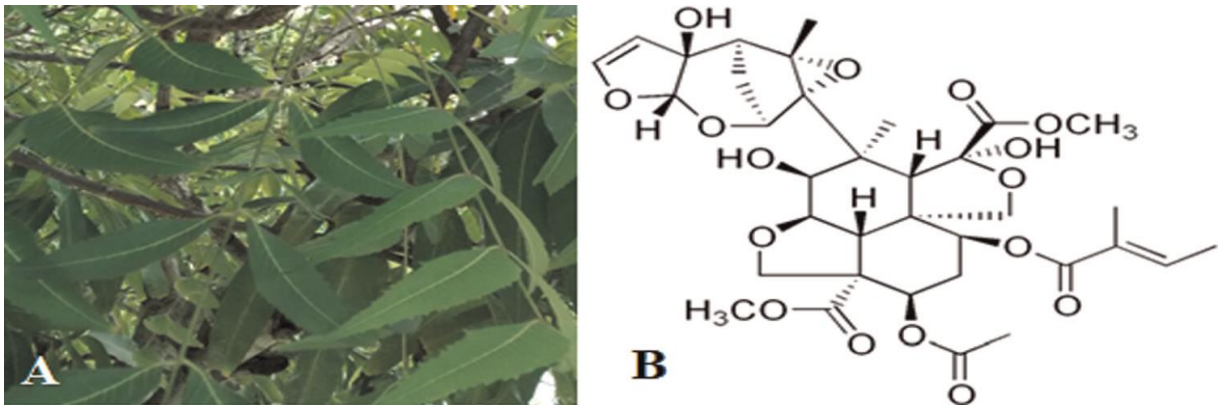

Figure 2b: (A) Leaves of neem (*Azadirachta indica*); (B) planar chemical structure of azadirachtin molecule

3.2.3 Preparation of Precursors and Synthesis of Pure and Cu doped Zinc Oxide Nanoparticles

3.2.3.1 Using Zinc Acetate Dihydrate [$Zn(CH_3COO)_2.2H_2O$]

Zinc acetate dihydrate [$Zn(CH_3COO)_2.2H_2O$] was used as precursor to synthesize ZnO nanoparticles using aqueous extract of neem leaf. 2M Zinc acetate solution was prepared by dissolving 109.75 g of Zinc acetate dihydrate in 250 mL double distilled water using 250 mL volumetric flask and stored for further use. 2M NaOH was prepared using double distilled water to be used as precipitating agent. Then four different samples were prepared by taking different ratios by volume of precursor salt solution and neem leaf extract.

Sample 1: $Zn(CH_3COO)_2.2H_2O$:Neem Leaf Extract (9:1) Ratio(45 mL:5mL) labeled as **ZAS_1**
Sample 2: $Zn(CH_3COO)_2.2H_2O$:Neem Leaf Extract (7:3) Ratio(35 mL:15mL) labeled as **ZAS_2**
Sample 3: $Zn(CH_3COO)_2.2H_2O$:Neem Leaf Extract (3:2) Ratio(30 mL:20mL) labeled as **ZAS_3**
Sample 4: $Zn(CH_3COO)_2.2H_2O$:Neem Leaf Extract (1:1) Ratio(25 mL:25mL) labeled as **ZAS_4**

$$Zn(CH_3COO)_2.2H_2O + \text{Plant extract} + 2NaOH \longrightarrow ZnO + 2NaOOCCH_3 + 3H_2O + \text{byproducts}$$

For sample 1: (9:1 Ratio)

5 mL of neem leaf extract and 45 mL of 2M NaOH were added to 45 mL of 2M $Zn(CH_3COO)_2.2H_2O$.

For sample 2: (7:3 Ratio)

15 mL of neem leaf extract and 35 mL of 2M NaOH were added to 35 mL of 2M $Zn(CH_3COO)_2.2H_2O$.

For sample 3: (3:2 Ratio)

20 mL of neem leaf extract and 30 mL of 2M NaOH were added to 30 mL of 2M $Zn(CH_3COO)_2.2H_2O$.

For sample 4: (1:1 Ratio)

25 mL of neem leaf extract and 25 mL of 2M NaOH were added to 25 mL of 2M $Zn(CH_3COO)_2.2H_2O$.

Then for each sample the mixture was stirred continuously for 2 hours with magnetic stirrer and resulted in solution with yellowish precipitate. The precipitate was filtered using Whatman filter paper No 1 and washed repeatedly with deionized water followed by ethanol in order to remove the impurities. Finally, the precipitate was dried in an oven at 60 ^{0}C for overnight and grinded to fine powder using agate mortar. The yellow powder obtained from the above method was calcined at 400 ^{0}C for 1 hour.

3.2.3.2 Using Zinc Nitrate Hexahydrate [$Zn(NO_3)_2.6H_2O$]

Zinc Nitrate hexahydrate [$Zn(NO_3)_2.6H_2O$] was used as precursor to synthesize ZnO nanoparticles using aqueous extract of neem leaf. 1 M zinc nitrate solution was prepared by dissolving 74.3725 g of Zinc Nitrate hexahydrate in 250 mL deionized water using 250 mL volumetric flask and stored in refrigerator and 2M NaOH was prepared in deionized water to be used as precipitating agent. Then 5 mL of neem leaf extract and 45 mL of 2 M NaOH were added to 45 mL of 1M $Zn(NO_3)_2.6H_2O$. Then the mixture was stirred continuously for 2 hours on magnetic stirrer resulting in white precipitate through the following reaction: (Tamanna Bhuyan, 2015).

$$Zn(NO_3)_2.\ 6H_2O + \text{Plant extract} + 2NaOH \longrightarrow ZnO + 2NaNO_3 + 7H_2O + \text{byproducts}$$

The precipitate was filtered using Whatman filter paper No 1 and washed repeatedly with deionized water followed by ethanol in order to remove the impurities. Finally, the precipitate was dried in an oven at 100 ^{0}C for 12 hour and grinded to fine powder using agate mortar (Daneshvar, 2008). The powder obtained from the above method was calcined at 400 ^{0}C for 1 hour.

3.2.3.3 Synthesis of Cu Doped ZnO Nanoparticles

For the preparation of $Zn_{1-x}Cu_xO$ nanopowder (x = 0.005, 0.01 and 0.015) the required stoichiometric amounts of zinc acetate and copper nitrate were dissolved with double distilled water separately and stored in refrigerator and the right ratio of the zinc acetate, copper nitrate and neem leaf extract were mixed at room temperature. For synthesis of Cu – doped ZnO

nanoparticles three samples were prepared using the stoichiometric amounts of zinc acetate and copper nitrate using the following molar ratios.

Sample 1: For x = 0.005 $\Rightarrow$ $Zn_{1-0.005}\ Cu_{0.005}O = Zn_{0.995}\ Cu_{0.005}O$ which is labeled as **CDS_1**

Sample 2: For x = 0.01 $\Rightarrow$ $Zn_{1-0.01}\ Cu_{0.01}O = Zn_{0.99}\ Cu_{0.01}O$ which is labeled as **CDS_2**

Sample 3: For x = 0.015 $\Rightarrow$ $Zn_{1-0.015}\ Cu_{0.015}O = Zn_{0.985}\ Cu_{0.015}O$ which is labeled as **CDS_3**

Synthesis of $Zn_{0.995}\ Cu_{0.005}O$ (CDS_1)

Cu – doped ZnO nanoparticles were synthesized by chemical precipitation method. In this case 4.13 x 10^{-2} moles of $Zn(CH_3COO)_2.2H_2O$ was dissolved in 90 mL of deionized water in 100 mL volumetric flask and 2.28 x 10^{-4} moles of $Cu(NO_3)_2.3H_2O$ was dissolved in 10 mL of deionized water (0.02077 M) in 25 mL volumetric flask.

Then 90 mL Zn $(CH_3COO)_2.2H_2O$ (0.46 M), 10 mL $Cu(NO_3)_2.3H_2O$ (0.02276 M) and 10 mL of neem leaf extract were mixed into 250 mL beaker. Then the mixture was stirred continuously using magnetic stirrer and the solution was kept at pH 7.0 by drop wise addition of 0.5 M sodium hydroxide (NaOH) with constant vigorous stirring with magnetic stirrer for 2 hours at room temperature. The obtained yellowish blue precipitate solution was separated from the solution by filtration using Whatman filter paper No 1. Then the resultant precipitant was washed repeatedly with deionized water followed by ethanol to eliminate the residual impurities in the sample and kept at 60 ^{0}C in hot air oven to get dried for 12 hours overnight. Finally, the powder was calcinated at 400 ^{0}C for 1 hour in Muffle furnace under air atmosphere to obtain Cu doped ZnO nanoparticles.

Synthesis of $Zn_{0.99}\ Cu_{0.01}O$ (CDS_2)

Cu – doped ZnO nanoparticles were synthesized by chemical precipitation method. In this case 4.10 x 10^{-2} moles of $Zn(CH_3COO)_2.2H_2O$ was dissolved in 90 mL of deionized water in 100 mL volumetric flask and 4.56 x 10^{-4} moles of $Cu(NO_3)_2.3H_2O$ was dissolved in 10 mL of deionized water (0.04138M) in 25 mL volumetric flask.

Then 90 mL $Zn(CH_3COO)_2.2H_2O$ (0.4552 M) , 10 mL $Cu(NO_3)_2.3H_2O$ (0.045 M) and 10 mL of neem leaf extract were mixed into 250 mL beaker. Then the mixture was stirred continuously using magnetic stirrer and the solution was kept at pH 7.0 by drop wise addition of 0.5 M sodium hydroxide (NaOH) with constant vigorous stirring on magnetic stirrer for 2 hours at room temperature. The obtained yellowish blue precipitate solution was separated from the solution by filtration using Whatman filter paper No 1. Then the resultant precipitant was washed repeatedly with deionized water followed by ethanol to eliminate the residual impurities in the sample and kept at 60 ^{0}C in hot air oven to get dried for 12 hours overnight. Finally, the powder was calcinated at 400 ^{0}C for 1 hour in Muffle furnace under air atmosphere to obtain Cu doped ZnO nanoparticles.

Synthesis of $Zn_{0.985}$ $Cu_{0.015}O$ (CDS_3)

Cu – doped ZnO nanoparticles were synthesized by chemical precipitation method. In this case 4.08 x 10^{-2} moles of $Zn(CH_3COO)_2.2H_2O$ was dissolved in 90 mL of deionized water in 100 mL volumetric flask and 6.83 x 10^{-4} moles of $Cu(NO_3)_2.3H_2O$ was dissolved in 10 mL of deionized water in 25 mL volumetric flask.

Then 90 mL $Zn(CH_3COO)_2.2H_2O$ (0.4531 M) , 10 mL $Cu(NO_3)_2.3H_2O$ (0.0683 M) and 10 mL of neem leaf extract were mixed into 250 mL beaker. Then the mixture was stirred continuously using magnetic stirrer and the solution was kept at pH 7.0 by drop wise addition of 0.5 M sodium hydroxide (NaOH) with constant vigorous stirring on magnetic stirrer for 2 hours at room temperature. The obtained yellowish blue precipitate solution was separated from the solution by filtration using Whatman filter paper No 1. Then the resultant precipitant was washed repeatedly with deionized water followed by ethanol to eliminate the residual impurities in the sample and kept at 60 ^{0}C in hot air oven to get dried for 12 hours overnight. Finally, the powder was calcinated at 400 ^{0}C for 1 hour in Muffle furnace under air atmosphere to obtain Cu doped ZnO nanoparticles.

3.3 Characterization Methods of Zinc Oxide Nanoparticles

3.3.1. Thermal Gravimetric Analysis (TGA)

Thermal gravimetric analysis (TGA) was carried out using a simultaneous DTA-TG apparatus (DTG-60H, Shimadzu Co., Japan) to determine the calcination temperature of the synthesized material. Approximately 8.475mg of the uncalcinated ZnO nanoparticle using zinc acetate precursor and 8.117 mg of uncalcinated Cu doped ZnO nanoparticle samples were placed in a platinum crucible on the pan of the microbalance and heated from room temperature to 1000 °C, using Al_2O_3 as inert material.

3.3.2. X-Ray Diffraction (XRD)

The crystalline structure of the green synthesized zinc oxide nanoparticles were investigated by the X-ray diffraction using X-ray diffractometer (Bruker D8 Advance Diffractometer). XRD spectrum was recorded from 10^0 to 80^0 with 2θ angles using CuKα (λ =1.54 Å) radiation operated at 40kV and 30 mA. Debye Scherrer's equation indicated in equation 1, was used to estimate the crystallite size.

$$D = \frac{0.94\lambda}{\beta cos\theta} \quad \text{.....(1)}$$

Where, D is the Crystallite size, λ is the X – ray source wavelength, β is the Full Width at Half Maximum (FWHM) of a peak, and θ is the Bragg diffraction angle.

3.3.3. Scanning Electron Microscopy (SEM)

In this research work JSM-6480 LV SEM machine was employed to study the morphology of synthesized nanoparticles. The experiment was performed at an accelerating voltage of 30 kV with a tilt angle of 45^o. The slide was coated with platinum and after the platinum coating, the SEM image was taken. In SEM characterization, nanoparticles powder is mounted on a sample holder followed by coating with a conductive metal. The sample is then scanned with focused fine beam of electrons. The surface characteristics of the sample are obtained from the secondary electrons emitted from the sample surface.

3.3.4. Energy Dispersive X- Ray Spectroscopy

The chemical composition of the green synthesized zinc oxide nanoparticles was estimated by energy-dispersive X-ray spectroscopy (EDX).

3.3.5. Fourier Transform Infrared (FT-IR) Spectroscopy

The synthesized ZnO nanoparticles were characterized by Perkin Elmer, 65 Spectrophotometer FT-IR Spectrum in order to analyze and detect surface functional groups at the scanning range of 4000 – 400 cm^{-1}. For the FT-IR characterization, the sample was mixed with solid KBr uniformly and properly, which was compressed to settle down on a thin transparent film and this thin transparent film was for FT-IR analysis which was kept in the chamber of the instrument for scanning.

3.3.6. UV-Visible Spectroscopy

The optical characterization of ZnO NPs was carried out using UV-Vis Spectroscopy (Perkin–Elmer lambda 950 UV/VIS/NIR/ spectrometer) in the wave length region of 260 nm - 1100 nm. First a dimethyl sulfoxide solvent was inserted in a 1 cm cuvette as a reference and the dimethyl sulfoxide solution and ZnO nanoparticles was placed in the second cuvette compartment for UV – Vis absorbance measurement.

3.4 Method for Antibacterial Activity

Materials used for antibacterial activity of pure and doped zinc oxide nanoparticles were Nutrient broth 1.3g, Nutrient agar 5.6g, Agar-agar 0.5g, petriplates, antibiotic discs, cotton swabs, zinc oxide nanoparticle sample, *Staphylococcus aureus*, *Bacillus subtilis*, *Escherichia coli* and *Proteus mirabilis*. Disc diffusion method was used for antimicrobial activity of zinc oxide nanoparticles.

3.4.1 Preparation of Inoculum

Nutrient broth (1.3 g in 100 mL deionized water) was prepared in 4 conical flasks and sterilized. In the first conical flask clinically isolated strain of *Staphylococcus aureus* and in the second conical flask clinically isolated strain of *Bacillus subtilis* were inoculated. In the third conical

flask clinically isolated strain of *Escherichia coli* and in the fourth conical flask clinically isolated strain of *Proteus mirabilis* were added. These bacterial cultures inoculated in nutrient broth will be kept on rotary shaker for 24 hours at 100 r.p.m.

3.4.2 Inoculation of Test Plate

Nutrient agar was prepared (5.6 g nutrient agar and 0.5g Agar-Agar in100 mL deionized water) and sterilized. The agar suspension within 15 min was used to inoculate plates by dipping a sterile cotton-wool swab into the suspension and remove the excess by turning the swab against the side of the container. Then the inoculum was spread evenly over the entire surface of the plate by swabbing in three directions. The plate was allowed to dry before applying to antibiotic discs.

3.4.3 Disc Diffusion Method for Antibacterial Activity

Antibacterial tests were carried out by the disc diffusion method using the suspension of bacteria spread on nutrient agar. Antibacterial activity of synthesized ZnO nanoparticles and Cu doped ZnO nanoparticles were tested against gram positive (*Staphylococcus aureus* and *Bacillus subtilis*) and gram negative (*Escherichia coli* and *Proteus mirabilis*) bacteria by disc diffusion method. In addition to this the antibacterial activity of Cu doped ZnO nanoparticles prepared in different ratios and uncalcined were tested against these bacterial strains. Bacterial cultures were maintained on nutrient Muller-Hinton agar at 37 ^{0}C and the cultures were kept in appropriate media slants and stored at 4 ^{0}C until used. The antibacterial activities were tested by the disc-diffusion agar method, which is a test of the antibiotic sensitivity of the bacteria and it uses the antibiotic discs to test the extent to which bacteria are affected by those antibiotics. Discs used for antibacterial activity were gentamicin, ciprofloxacin and erythromycin. The antibiotic gentamicin was used as control. Discs were applied to the surface of an agar plate that was previously dried. The plates were then turned upside down and incubated at 37^0 C for 24 h in an incubator. The plates were shaken gently to allow evenly mixing of bacteria cells and agar. A 60 mm plate accommodated two discs and ZnO nanoparticles without unacceptable overlapping of zones. Agar plate was divided into 3 sections antibiotic disc, zinc oxide nanoparticles sample,

and both antibiotic disc and zinc oxide nanoparticle sample. Then 200 mg of ZnO nanoparticles using zinc nitrate and zinc acetate precursors and 100 mg of Cu doped ZnO nanoparticles were dissolved in 20 mL and 10 mL of de-ionized water, respectively, to obtain each 10 mg/mL. From each sample, 200 µL of each concentration saturated with discs (6 mm diameter disc) was placed on plate and incubated at 37 ^{0}C for 24 hours. The diameters of the inhibition zones were calculated. Clear inhibition zones formed around the discs indicated the presence of antibacterial activity. The results were taken by considering the zone of growth and inhibition of the bacteria by the test fractions. Antibacterial activity was evaluated by measuring the diameter (mm) of the inhibition zone (IZ) around the disc against the test organisms by using a ruler.

4. RESULTS AND DISCUSSION

In this section, we mainly presented the characterization of Zinc oxide and copper doped zinc oxide nanoparticles synthesized by biological method from zinc acetate and copper nitrate, and their application for antibacterial activity.

4.1. Thermal Gravimetric Analysis (TGA)

The uncalcinated synthesized ZnO nanoparticles using zinc acetate precursor (UZAS1) and Cu-doped ZnO nanoparticles (UCDS1) were characterized by using TGA/DTA (Differential Thermal Analysis). The weight losses of the investigated materials were analyzed. Figure 3 shows the thermo gravimetric analysis (TGA) and differential thermal analysis (DTA) of the uncalcined ZnO nanoparticles using zinc acetate precursor (UZAS1). TGA curve shows mass loss of the sample whereas DTA curve indicates the energy gain or loss during the process. TGA/DTA transition shows a loss of 14.667 % up to 400 ^{0}C. No considerable loss is observed after this up to 1000 ^{0}C. TGA-DTA data for $Zn(OH)_2$ precursor registered strong endothermic peak at 400 ^{0}C. This indicates that after 400 ^{0}C there is no weight loss for the synthesized ZnO nanoparticles and the nanoparticle is thermally stable. This temperature was used for calcination of the synthesized ZnO nanoparticles using zinc acetate precursor.

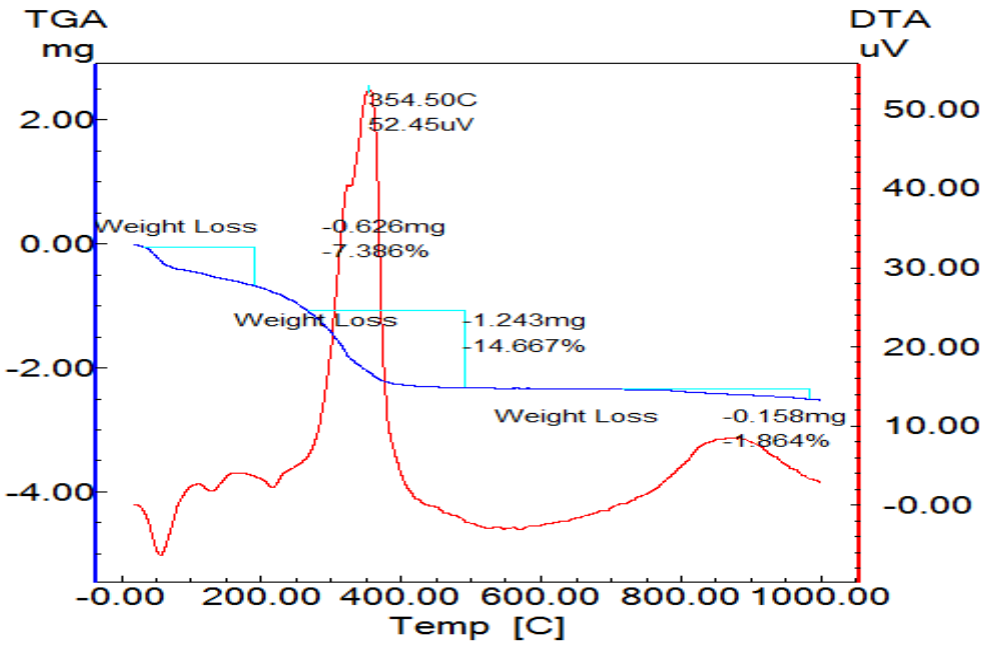

Figure 3: Thermal Analysis result for uncalcinated ZnO NPs using zinc acetate (UZAS1).

Figure 4 shows the thermo gravimetric analysis (TGA) of the uncalcinated $Zn_{0.995}Cu_{0.005}O$ (UCDS1). Weight loss continues up to 400 ^{0}C, but it stays constant after 400 ^{0}C. After this temperature there is no considerable loss in mass is observed up to 1000 ^{0}C. This indicates that after 400 ^{0}C there is no significant weight loss for the synthesized Cu doped ZnO nanoparticles. So, the mass loss ends at about 400 ^{0}C and this temperature was also used for calcination of the synthesized UCDS1. As the TGA and DTA was carried out before calcination of the sample DTA curve shows strong endothermic peak at 400 ^{0}C might be due to the decomposition reaction.

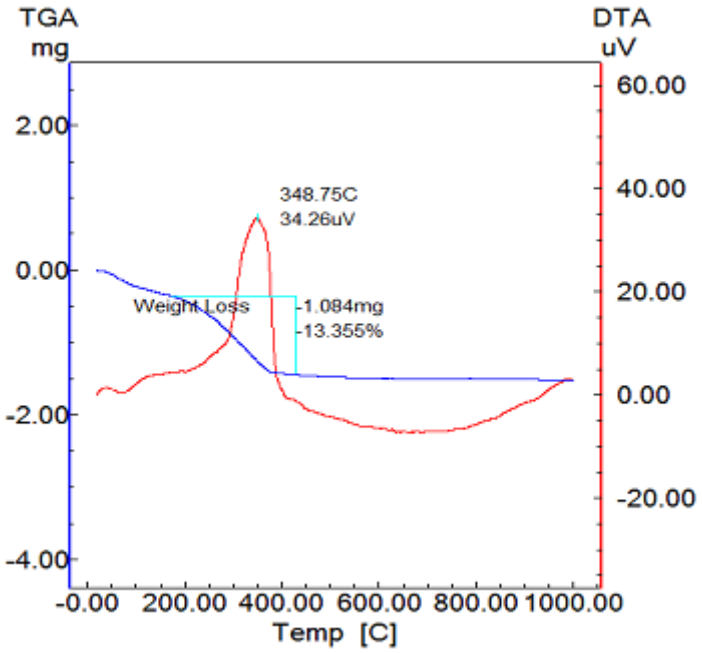

Figure 4: Thermal Analysis result for uncalcinated $Zn_{0.995}Cu_{0.005}O$ (UCDS1).

4.2. X-Ray Diffraction (XRD)

Figure 5 (a and b) shows the XRD patterns of ZnO NPs synthesized from zinc nitrate and zinc acetate precursors while Figure 5 (c and d) shows the XRD patterns of Cu doped ZnO NPs for $Zn_{0.995}Cu_{0.005}O$ and $Zn_{0.985}Cu_{0.015}O$ respectively, which were synthesized using stoichiometric amounts of zinc acetate and copper nitrate salts.

As indicated on Figure 5 the ZnO NPs peaks from zinc nitrate are observed at 2θ 32.04, 34.72, 36.53, 47.65, 56.86, 63.19, 68.27 and 69.37^{o} and from zinc acetate are at 31.91, 34.57, 36.40, 47.71, 50.85, 56.75, 63.06 and 68.16^{o} and their corresponding crystal size is given in Table 4. Even if the two materials were prepared by the same procedure, there is a slight shift of 2θ position for certain peaks. This might be due to the different zinc precursors used. The average crystalline size calculated using Debye- Scherrer equation of the diffraction peak was found to be 22.93 nm and 23.74 nm for zinc nitrate and zinc acetate precursors, respectively.

The crystal structure of $Zn_{1-x}Cu_xO$ samples with value of x = 0.005 and 0.015 shown in Figure 5 (c and d, respectively) were determined by X-ray diffractometer in the range of 10^{o} to 70^{o} at room temperature. All the indexed diffraction peaks were match with the hexagonal phase ZnO reported in JCPDS card No 36-1451(with a = 0.3249 nm, c = 0.5206 nm). The sharp intense peak obtained in all samples at 2θ ≈ 28.77, 31.98, 34.63, 36.46, 47.72, 56.81, 63.12 and 68.22^{o} corresponds to the lattice plane (001), (100), (002), (101), (102), (110), (103) and (112) respectively confirms that the prepared samples are good crystalline in nature with wurtzite hexagonal structure (C. Chen, 2007). The average crystalline size of Cu doped ZnO NPs for $Zn_{0.995}Cu_{0.005}O$ and $Zn_{0.985}Cu_{0.015}O$ was found to be 18.36 nm and 16.07 nm respectively. Here Cu doped ZnO nanoparticles have smaller crystalline size than pure ZnO nanoparticles.

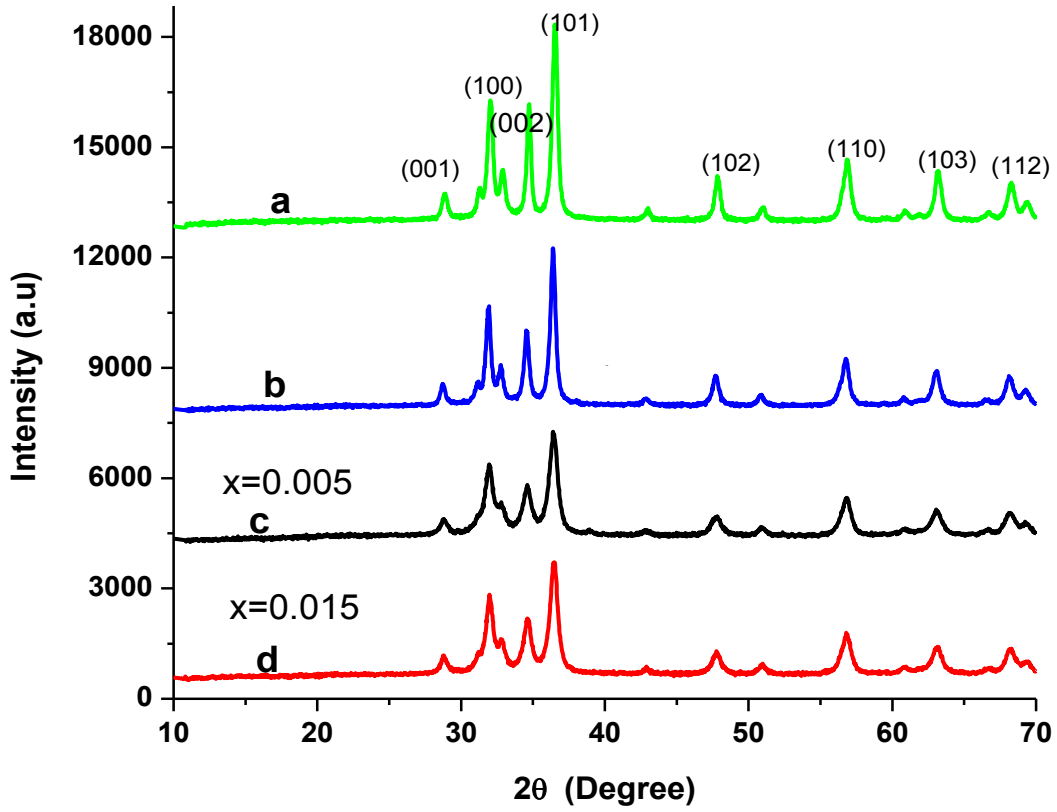

Figure 5: XRD pattern of ZnO NPs synthesized from (a) Zinc nitrate, (b) zinc acetate, and $Zn_{1-x}Cu_xO$ samples with (c) $Zn_{0.995}Cu_{0.005}O$ and (d) $Zn_{0.985}Cu_{0.015}O$

The difference in crystal size may be due to difference in precursors used for making ZnO NPs. All diffraction peaks of samples correspond to the characteristic hexagonal wurtzite structure of zinc oxide nanoparticles by comparison with the data from JCPDS card 36-1451with lattice parameters (a = 3.2493 Å and c = 5.2056 Å) (N. Srinivasa Rao, 2015; S. Jurablu, 2015; S.S. Kulkarni, 2015; N. Rajagopalan, 2013). For Cu doped ZnO the values of lattice parameters are a = 3.2504 Å and c = 5.2060 Å. A definite line broadening of the diffraction peaks also resembles that the synthesized particles are in nanometer range and no characteristic peaks were observed other than ZnO peaks, confirming the high purity of the synthesized products (N. Srinivasa Rao, 2015).

No additional peaks corresponding to the secondary phases of copper oxides or impurity were obtained for x=0.005 to 0.015 at 400^0 C, which indicates that the wurtzite structure is not disturbed by the Cu substitution. Thus, we conclude that the doping of Cu does not change the wurtzite structure of ZnO and hence Cu^{2+} substitutes Zn^{2+} in the crystal lattice. No other peaks corresponding to Cu related secondary or impurity phase was found in copper doped sample, which may be attributed to the incorporation of Cu ion into the Zn lattice site rather than interstitial ones.

Table 1 shows the results of d – spacing (d_{hkl}) and Miller indices (h k l) for pure ZnO nanoparticles calculated using POWD – an Interactive Powder Diffraction Data Interpretation and Indexing program version 2.2 software.

Table 1: d – spacing ($d_{h\,k\,l}$) and Miller indices for ZNS1 and ZAS1

For ZnO nanoparticle using Zinc nitrate(**ZNS1**)			For ZnO nanoparticle using zinc acetate(**ZAS1**)		
2θ(degree)	d – spacing ($d_{h\,k\,l}$) (Å)	Miller Indices h k l	2θ(degree)	d – spacing ($d_{h\,k\,l}$) (Å)	Miller Indices h k l
32.04	2.7911	1 0 0	31.91	2.8021	1 0 0
34.72	2.5815	0 0 2	34.57	2.5924	0 0 2
36.53	2.4576	1 0 1	36.40	2.4661	1 0 1
47.65	1.9068	1 0 2	47.71	1.9046	1 0 2
56.86	1.6179	1 1 0	50.85	1.7941	0 0 3
63.19	1.4702	1 0 3	56.75	1.6208	1 1 0
68.28	1.3725	1 1 2	63.06	1.4729	1 0 3
69.37	1.3535	2 0 1	68.16	1.3746	1 1 2

The XRD pattern of ZnO nanoparticles using zinc acetate and neem leaf extract in 1:1 ratio was studied and the sharp intense peak obtained at 2θ ≈ 32.17, 34.82, 36.65, 47.96, 51.11, 56.99, 63.29 and 68.39^o corresponds to the lattice plane (100), (002), (101), (102), (003), (110), (103) and (112), respectively. All the diffraction peaks can be well indexed to the hexagonal phase ZnO reported in JCPDS card (No. 36-1451, a = 0.3249 nm, c = 0.5206 nm). Diffraction peaks

related to impurities were not observed in the XRD pattern, confirming the high purity of the product synthesized. Furthermore, it could be seen that the diffraction peaks shown in Figure 6 were more intensive and narrower, implying the good crystalline nature of the synthesized ZnO product. The average crystalline size (D) of the nano-sized ZnO particles was estimated to be about 19.8 nm according to the Debye-Scherrer formula.

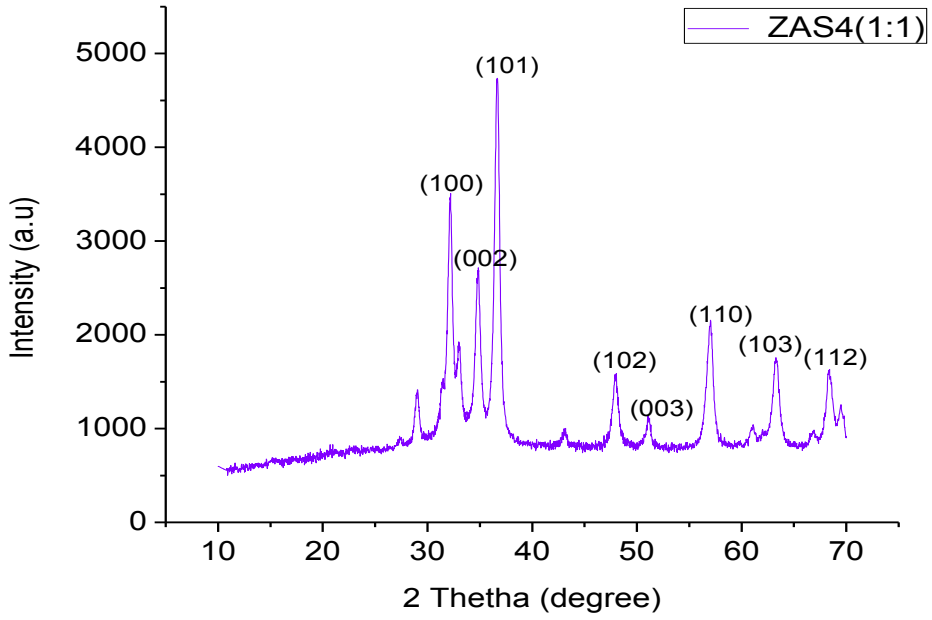

.

Figure 6: XRD pattern for ZnO nanoparticles synthesized using zinc acetate and Neem leaf extract (1:1)

As compared to ZnO nanoparticles synthesized using zinc acetate and neem leaf extract in 9:1 ratio, XRD result showed that the average crystallite size of ZnO nanoparticles in 1:1 ratio has a smaller particle size. This difference may be due to the greater amount of leaf extract used during synthesis process resulting in more capping agents that inturn effectively stabilize the synthesized nanoparticles.

Table 2: FWHM values, Crystallite sizes, d–spacing ($d_{h\,k\,l}$) and Miller indices for ZAS4 (1:1)

2θ (degree)	FWHM (degree)	Crystallite size (nm)	d-spacing (Å)	Miller Indices h k l
32.17	0.4062	21.26	2.7801	1 0 0
34.82	0.4378	19.73	2.5743	0 0 2
36.65	0.4488	19.48	2.4499	1 0 1
47.96	0.4967	18.28	1.8952	1 0 2
51.11	0.3387	27.16	1.7856	0 0 3
56.99	0.5569	16.95	1.6145	1 1 0
63.29	0.5414	18	1.4681	1 0 3
68.39	0.5776	17.5	1.3705	1 1 2
Average Crystallite size		**19.8**		

Table 3 shows the results of d – spacing ($d_{h\,k\,l}$) and Miller indices (h k l) for Cu doped ZnO nanoparticles calculated using POWD – an Interactive Powder Diffraction Data Interpretation and Indexing program version 2.2 software.

Table 3: d – spacing ($d_{h\,k\,l}$) and Miller indices for CDS1 and CDS3

For $Zn_{0.995}Cu_{0.005}O$ (**CDS1**)			For $Zn_{0.985}Cu_{0.015}O$ (**CDS3**)		
2θ(degree)	d – spacing ($d_{h\,k\,l}$) (Å)	Miller Indices h k l	2θ(degree)	d – spacing ($d_{h\,k\,l}$) (Å)	Miller Indices h k l
31.99	2.7953	1 0 0	31.96	2.7979	1 0 0
34.63	2.5880	0 0 2	34.60	2.5902	0 0 2
36.46	2.4622	1 0 1	36.43	2.4642	1 0 1
47.77	1.9023	1 0 2	47.74	1.9034	1 0 2
50.94	1.7911	0 0 3	50.92	1.7918	0 0 3
56.82	1.6189	1 1 0	56.80	1.6195	1 1 0
63.12	1.4717	1 0 3	63.08	1.4725	1 0 3
68.22	1.3735	1 1 2	68.20	1.3739	1 1 2

Table 4: Different angles and their corresponding FWHM values and sizes of ZnO NPs using zinc nitrate and zinc acetate precursors

2θ(degree)	FWHM(degree)	Size of ZnO NPs using zinc nitrate(nm)	2θ (degree)	FWHM(degree)	Size of ZnO NPs using zinc acetate(nm)
32.04	0.3805	22.62	31.91	0.3144	27.3
34.72	0.2849	30.8	34.57	0.2901	30
36.53	0.3816	22.88	36.40	0.3237	27
47.65	0.4150	21.87	47.71	0.3920	23
56.86	0.4157	22.69	50.85	0.3769	24.37
63.19	0.4480	21.74	56.75	0.4665	20.21
68.28	0.4701	21.3	63.06	0.4806	20.26
69.37	0.5168	19.56	68.16	0.5626	17.81
Average crystallite size		**22.93**	Average crystallite size		**23.74**

Table 5: Different angles and their corresponding FWHM values and sizes of Cu doped ZnO NPs using zinc acetate and copper nitrate precursors

2θ(degree)	FWHM (degree)	Size of Cu doped ZnO NPs ($Zn_{0.995}Cu_{0.005}O$)(nm)	2θ (degree)	FWHM (degree)	Size of Cu doped ZnO NPs($Zn_{0.985}Cu_{0.015}O$)(nm)
31.99	0.4466	19.33	31.96	0.4417	19.53
34.63	0.4482	19.40	34.60	0.4907	17.72
36.46	0.4717	18.51	36.43	0.5512	15.84
47.77	0.5756	15.83	47.74	0.6861	12.06
50.94	0.4964	18.51	50.92	0.6507	14.05
56.82	0.5130	18.39	56.80	0.5754	16.45
63.12	0.6158	18.97	63.08	0.6313	15.45
68.22	0.5583	17.96	68.20	0.5766	17.48
Average crystallite size		**18.36**	Average crystallite size		**16.07**

4.3. Scanning Electron Microscopy (SEM) Analysis

The morphology of ZnO nanoparticles were studied using SEM images. The surface morphology of the synthesized samples was viewed through the high resolution scanning electron microscope. SEM images of ZnO NPs have different morphology as shown in Figure 7 (a-e). The morphology of uncalcined ZnO as indicated in Figure 7 (a) is not clearly identified. The SEM images of calcined ZnO and Cu doped ZnO on (Figure 7(b - e) indicate the agglomeration of particles that increases with the concentration of zinc acetate. The morphology of ZnO NPs synthesized from zinc acetate in different mixing ratio of reactants such as 9:1, 7:3 and 3:2 have agglomerated spherical shapes. On the SEM image of Cu doped ZnO ($Zn_{0.985}Cu_{0.015}O$), Figure 7 (e), cluster, flake-like and agglomerated spherical shapes were observed. The scanning electron microscope results confirmed that the grain sizes of the synthesized NPs were strongly dependent on mixing ratio of Zinc acetate & leave extracts under the same reaction conditions.

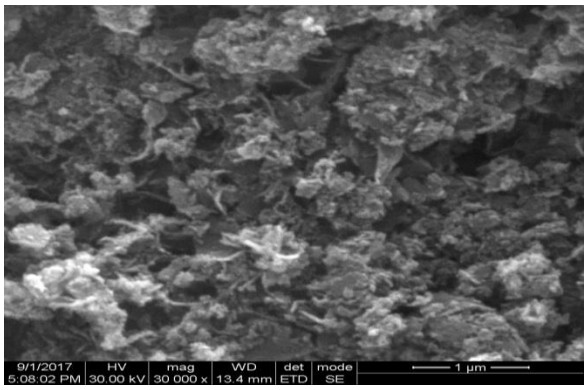

(a)

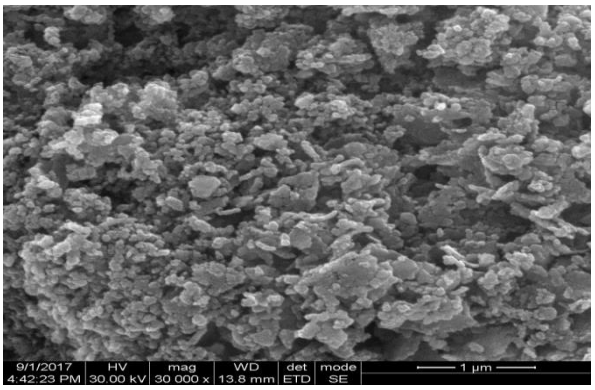

(b)

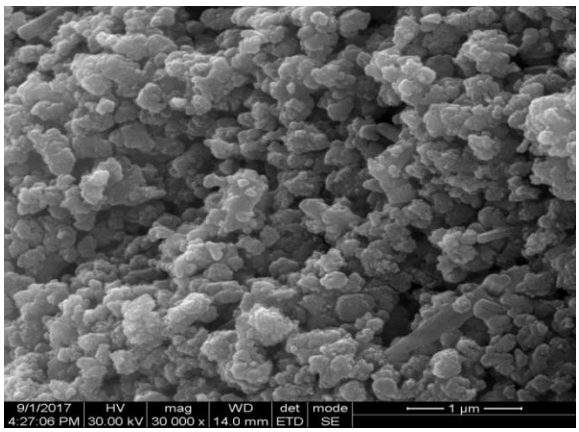

(c)

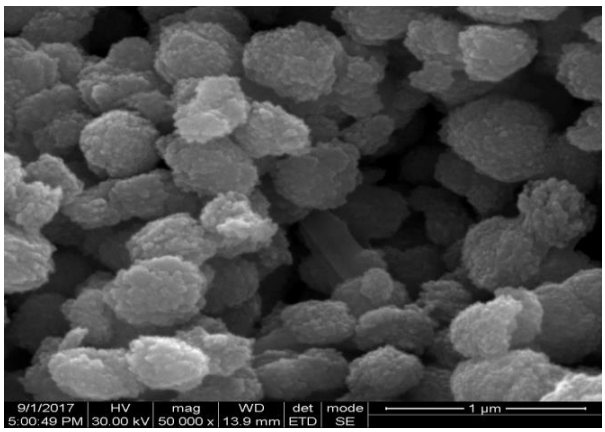

(d)

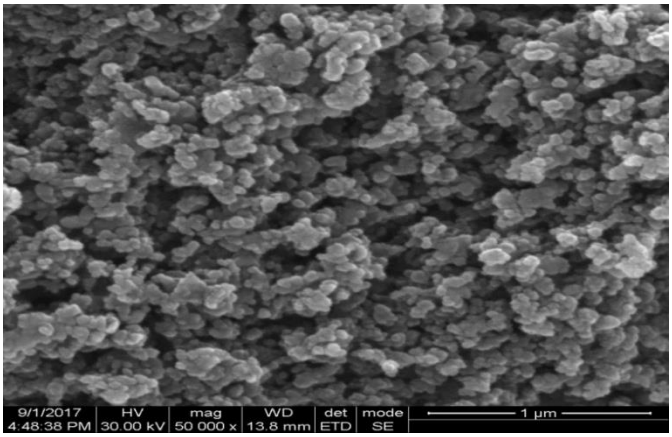

(e)

Figure 7: SEM images of ZnO Nanoparticles for: (a) Uncalcinated ZnO using zinc acetate (9:1), (b) Calcined ZnO using zinc acetate (9:1), (c) Calcined ZnO using zinc acetate (7:3), (d) Calcined ZnO using zinc acetate (3:2) and (e) Calcined Cu doped ZnO ($Zn_{0.985}Cu_{0.015}O$)

The SEM image results also agreed with XRD results obtained, i.e. the crystal sizes in XRD with big size have also big shapes in SEM images. This indicates that ZnO NPs have successfully prepared using zinc acetate precursor within a nano range. The SEM images clearly show micro structural homogeneities and remarkably different morphology for ZnO powder.

4.4. Energy Dispersive X-Ray Spectroscopy (EDX) Analysis

The composition of the samples was determined by energy dispersive X-Ray spectroscopy (EDX) using scanning microscope. The energy dispersive X-ray analysis of all ZnO nano particles using zinc acetate at different mixing ratios are shown in Figures 8 to 15. It is evident from the X-ray patterns of all the samples in which Zn and O are found in the respective spectrum. In addition to that interestingly it is observed there is no foreign material present in the spectrum. It is added confirmation for the purity of the samples. Quantitative analyses of the samples are indicated in the Tables 6 - 9. Also in the tables it is seen that no impurities are found out.

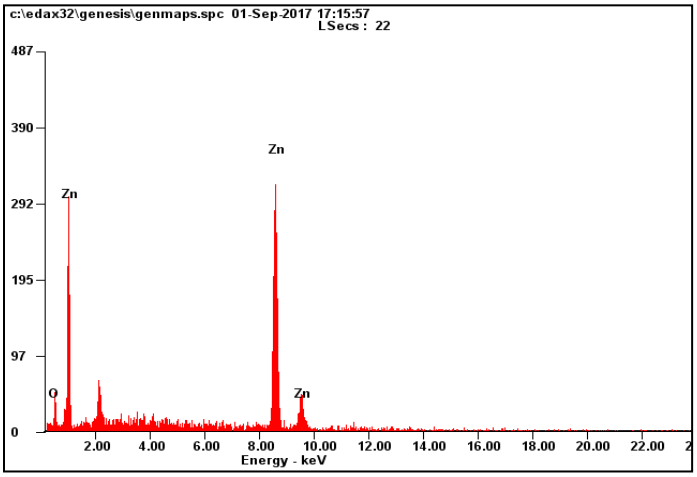

Figure 8: EDX spectrum of ZAS1(9:1)

In Table 6, ZAF refers to matrix correction: Z = atomic number correction, A = Absorption correction, F = Fluorescence correction. The weight percent for zinc and oxygen were 88.91 and 11.09 respectively giving a total of 100 %.

Table 6: Quantitative analysis of ZAS1(9:1)

Element	*Wt%*	*At%*
OK	11.09	33.77
ZnK	88.91	66.23
Matrix	Correction	ZAF

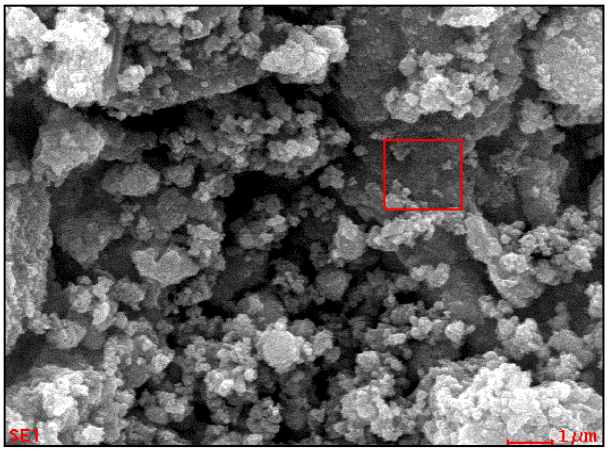

Figure 9: SEM images of selected area for EDX spectra of ZAS1

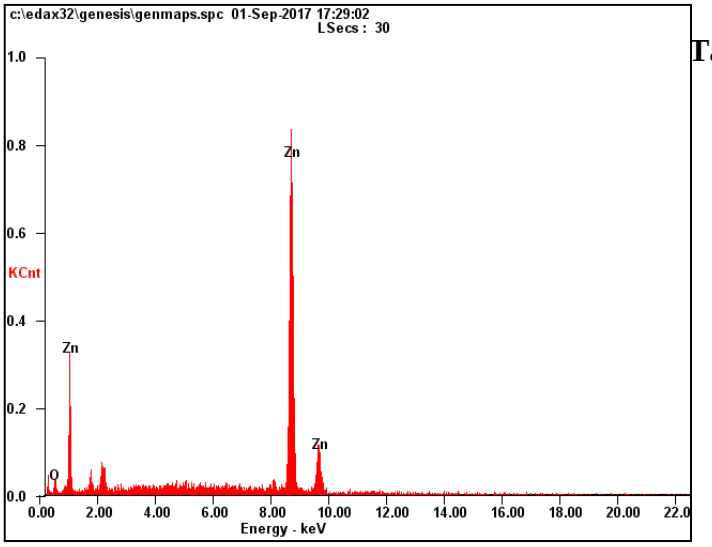

Figure 10: EDX Spectrum of ZAS2(7:3)

Table 7: Quantitative analysis of ZAS2(7:3)

Element	*Wt%*	*At%*
OK	20.85	51.83
ZnK	79.15	48.17
Matrix	Correction	ZAF

From Table 7, the weight percent for zinc and oxygen were 79.15 and 20.85 respectively giving 100 %. Their atomic percent are 48.17 and 51.83 respectively giving a total of 100 %.

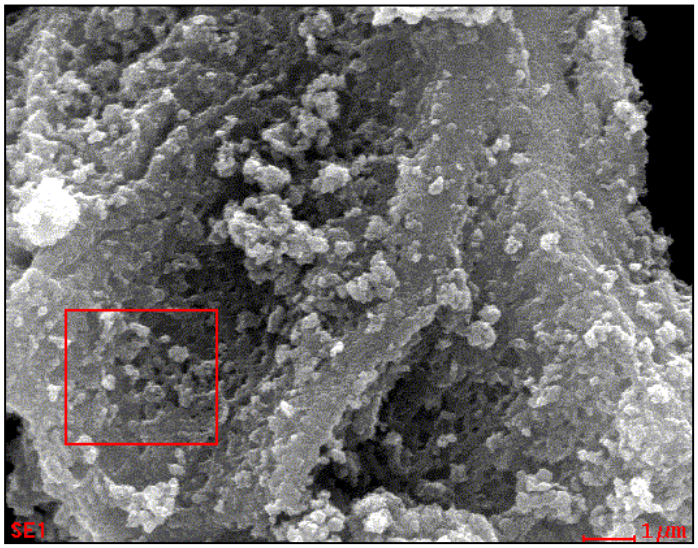

Figure 11: SEM images of selected area for EDX spectra of ZAS2

In Figure 10, the EDX spectrum of ZnO nanoparticles for 7:3 ratio showed that the sample contains the elements zinc and oxygen. In Table 7, the weight and atomic percent for the elements were given. From the results EDX spectrum shows that the well agreement with experimental concentration elemental composition of ZnO nanoparticles.

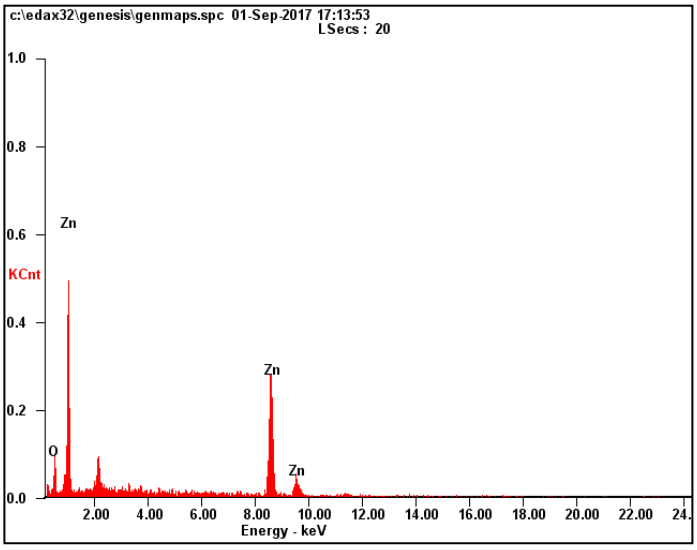

Figure 12: EDX Spectrum of ZAS3(3:2)

Table 8: Quantitative analysis of ZAS3(3:2)

Element	*Wt%*	*At%*
OK	15.25	42.38
ZnK	84.75	57.62
Matrix	Correction	ZAF

From Table 8, the weight percent for oxygen and zinc were 15.25 and 84.75 % respectively giving a total of 100 %. Their atomic percent were 42.38 and 57.62 respectively giving a total of 100 %.

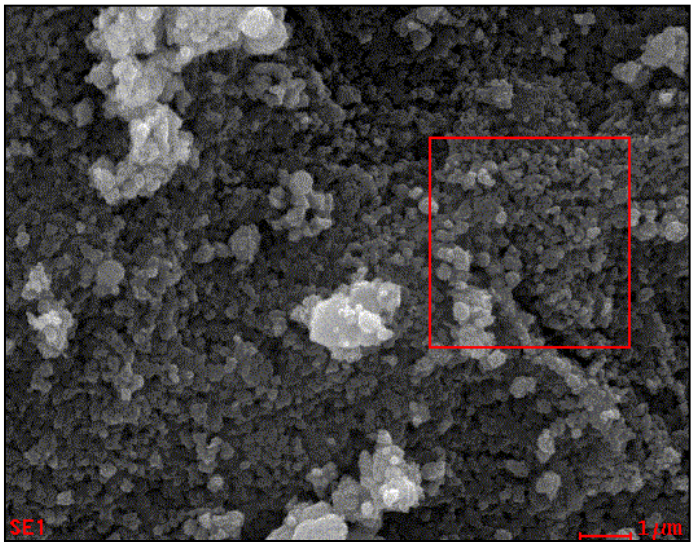

Figure 13: SEM images of selected area for EDX spectra of ZAS3

The EDX spectrum (From Figure 8, 10 and 12) shows that in all samples of pure ZnO nanoparticles which were synthesized using zinc acetate at different ratios zinc and oxygen signals have been detected, suggesting that the nanoparticle is only made up of Zn and O. The energy dispersive spectra of the samples obtained from the SEM-EDX analysis (Figure 12) clearly show that the sample prepared by the above route has pure ZnO phases.

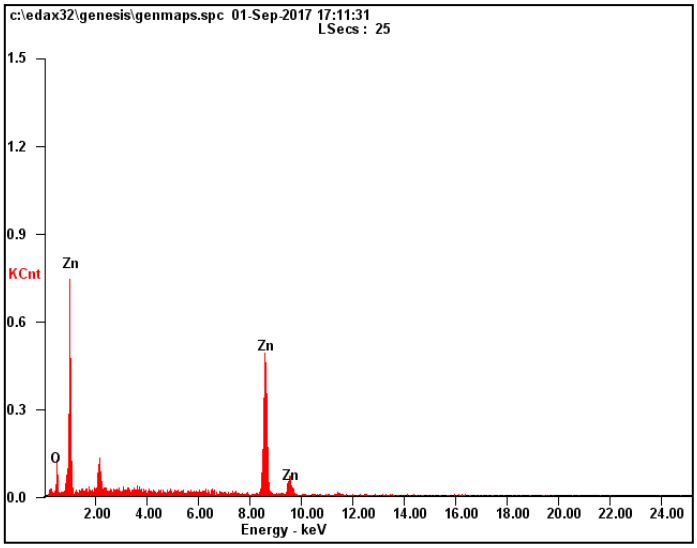

Figure 14: EDX Spectrum of CDS3 ($Zn_{0.985}Cu_{0.015}O$)

Table 9: Quantitative analysis of CDS3

Element	*Wt%*	*At%*
OK	04.68	16.70
ZnK	95.32	83.30
Matrix	Correction	ZAF

From Table 9, the weight percent for the elements oxygen and zinc were 4.68 and 95.32 % respectively giving a total of 100 %. Their atomic percent were 16.70 and 83.30 % respectively giving a total of 100 %.

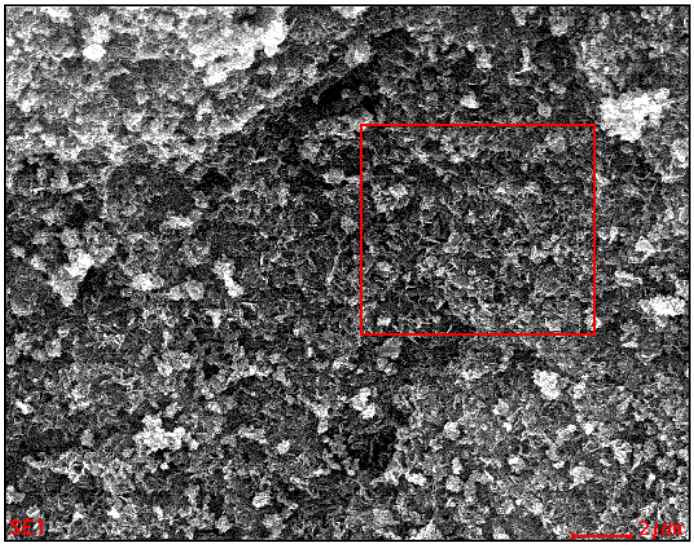

Figure 15: SEM images of selected area for EDX spectra of CDS3 ($Zn_{0.985}Cu_{0.015}O$)

Figure 14 gives the elemental spectra of ZnO nanoparticles exposed by EDX analysis for Cu doped ZnO nanoparticles ($Zn_{0.985}Cu_{0.015}O$). It specifies that the ZnO wurtzite structure is only composed of two elements Zinc and Oxygen. In the spectra the element copper was not observed. This could be due to the smaller concentration of copper during doping. Figure 15 shows the SEM image and selected area for EDX spectra analysis for doped sample.

4.5. Fourier Transformed Infrared (FT-IR) Spectroscopy Analysis

This FT-IR gives information on the vibrational and rotational modes of motion of a molecule and hence an important technique for identification and characterization of a substance. The Infrared spectrum of an organic compound provides a unique fingerprint, which is readily distinguished from the absorption patterns of all other compounds; only optical isomers absorb in exactly the same way. Hence FT-IR is an important technique for identification and characterization of a substance.

The vibrational phonon and the quality of ZnO NPs were characterized by Fourier Transformed Infrared (FT-IR) (Perkin Elmer, 65) in the wave number range of 400-4000 cm^{-1}. Measurements of ZnO NPs were performed by putting the powder of ZnO NPs on KBr plate.

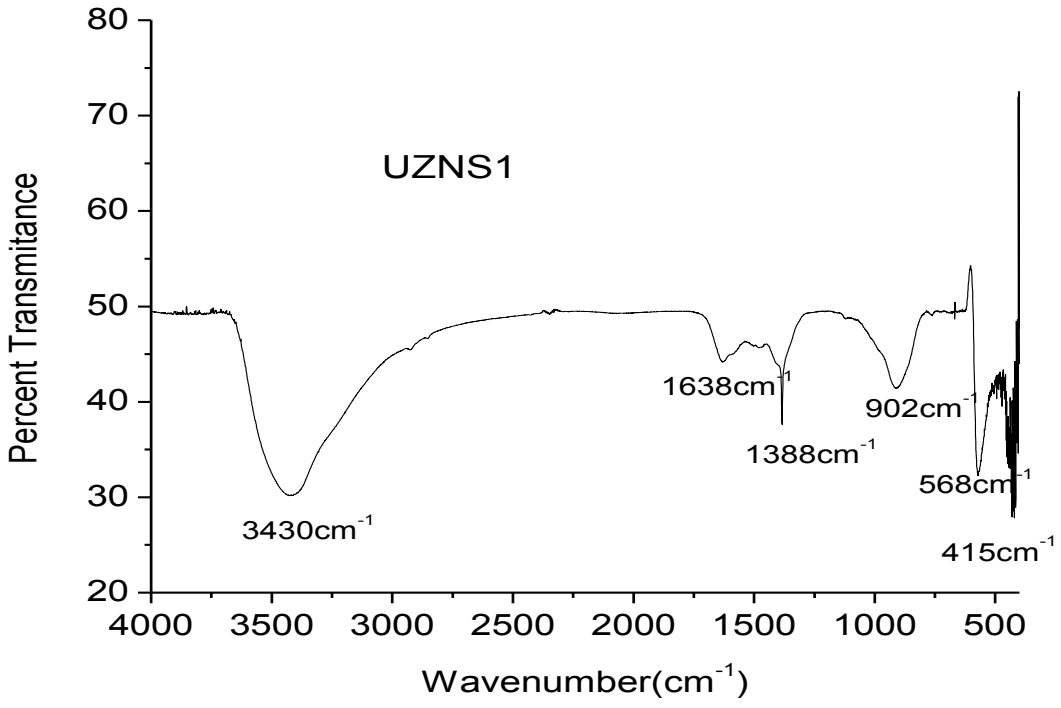

Figure 16: FT-IR spectrum for uncalcinated ZnO NPs synthesized using zinc nitrate precursor

Figure 16 Shows the FT-IR spectra of the green synthesized ZnO NPs using zinc nitrate before calcination. In the spectrum, the wide absorption around 3430 cm^{-1} is caused by the presence of an O-H stretching vibrations due to the absorbed water on the surface of the samples. C=O vibrations are observed around 1638 cm^{-1}, N=O vibrations occur around 1388 cm^{-1} and at 902 cm^{-1} – COOH bending vibrations of carboxylic acid functional groups are observed. As it can be seen in Figure 16, the intense absorption peak at 415-568 cm^{-1} is related to the stretching vibrations of Zn–O bond.

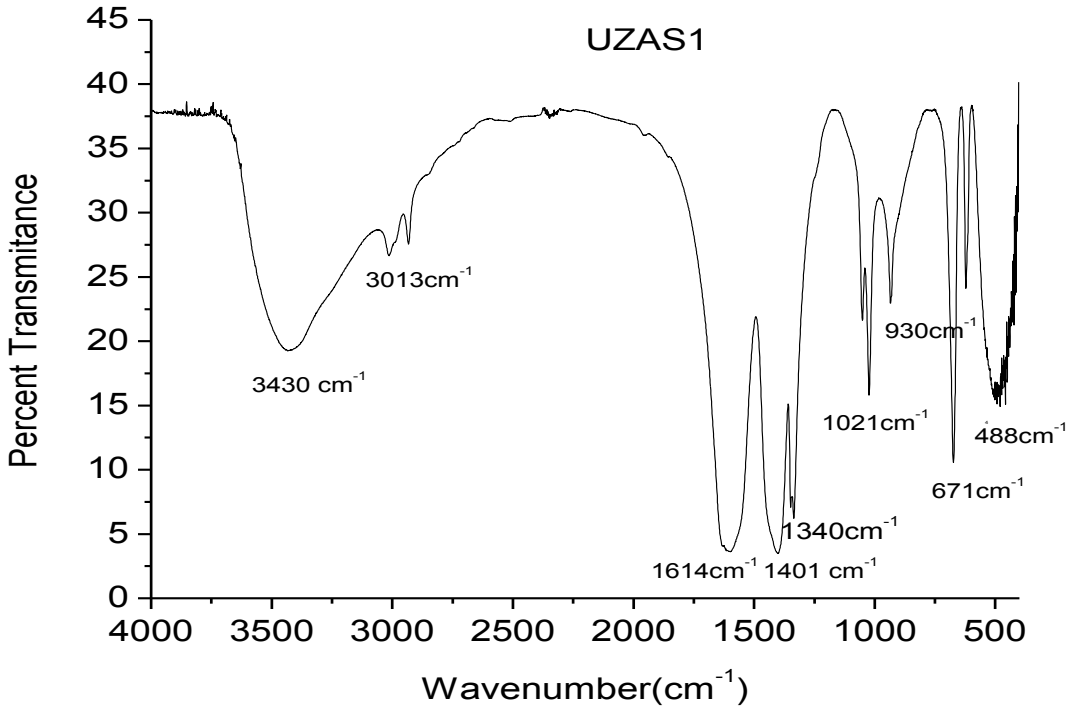

Figure 17: FT-IR spectrum for uncalcinated ZnO NPs synthesized using zinc acetate precursor

Figure 17 Shows the FT-IR spectra of the green synthesized ZnO NPs using zinc acetate before calcinations. In the spectrum, the wide absorption around 3430 cm^{-1} is due to O-H stretching vibrations. The two bands which occur around 3013 cm^{-1} is due to N-H stretching vibrations. Aromatic C=C ring stretching absorption occurs around 1614 cm^{-1}. Strong intensity at 1401 cm^{-1} is due to α-CH_2 bending vibrations of aldehydes and ketones. In the spectrum, the medium

intensity around 1340 cm^{-1} is due to O-H bending. C-O stretching vibrations are observed around 1021 cm^{-1}. C-O-H bending occurs around 930 cm^{-1}. As it can be seen in Figure 17, the intense absorption peak at 488 cm^{-1} is related to the stretching vibrations of Zn–O bond.

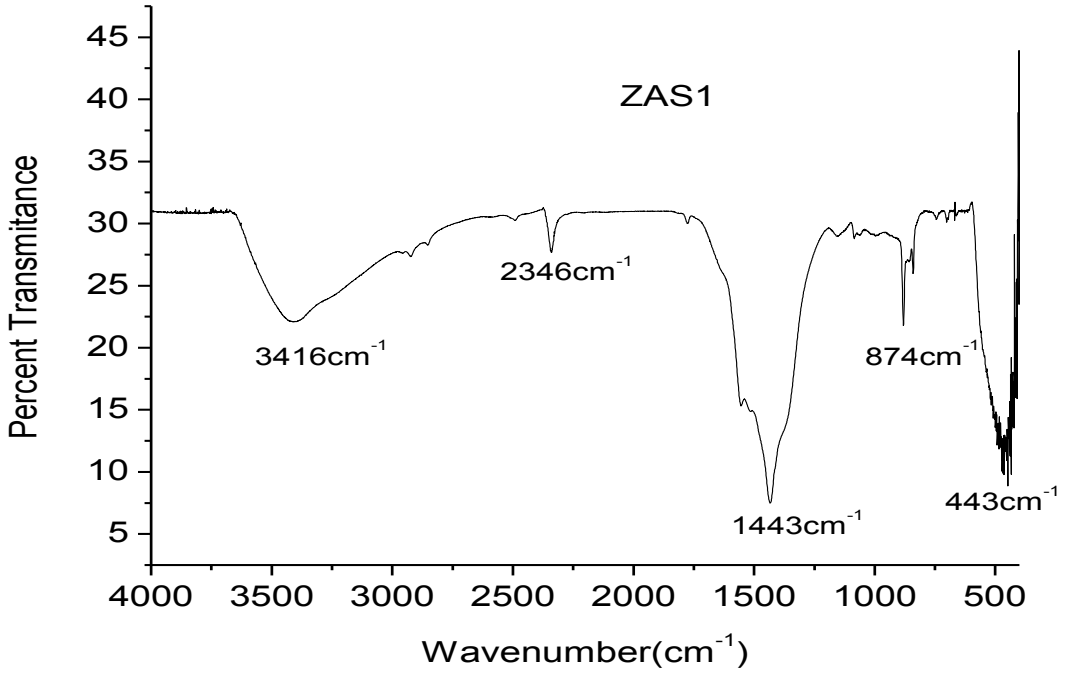

Figure 18: FT-IR spectrum for calcinated ZnO NPs synthesized using zinc acetate precursor

Figure 18 Shows the FT-IR spectra of the green synthesized ZnO NPs using zinc acetate after calcinations of a temperature at 400 ^0C. In the spectrum, the wide absorption around 3410 cm^{-1} is due to O-H stretching vibrations. The absorption at 2340 cm^{-1} is because of the presence of CO_2 molecules in the environment (Gayen R.N. & A.K., 2008). Strong intensity around 1443 cm^{-1} is due to α-CH_2 bending vibration. Strong peak at 874 cm^{-1} is due to the C–H bending frequency. As it can be seen in Figure 18, the intense absorption peak at 443 cm^{-1} is related to the stretching vibrations of Zn–O bond. As compared to calcined ZnO NPs the FT-IR spectra of uncalcined ZnO NPs (Figure 17) displayed a number of absorption peaks. This might be due to chemically bonded functional groups of neem leaf extract used as a capping agent during the synthesis of the materials which was not removed by washing with deionized water and ethanol.

The FT-IR spectra of the white powder produced after calcinations at 400 ^{0}C for 1 h (Figure 18) exhibited strong absorption bands around 410–480 cm^{-1}, confirming the Zn–O stretching frequencies. Furthermore, the peaks intensity of –COOH group in 1400–1600 cm^{-1} was relatively reduced, indicating the removal of the organic compound from ZnO nanoparticles. The organic compound in plant extract could stabilize nanoparticles by the surface binding (Iravani, 2011).

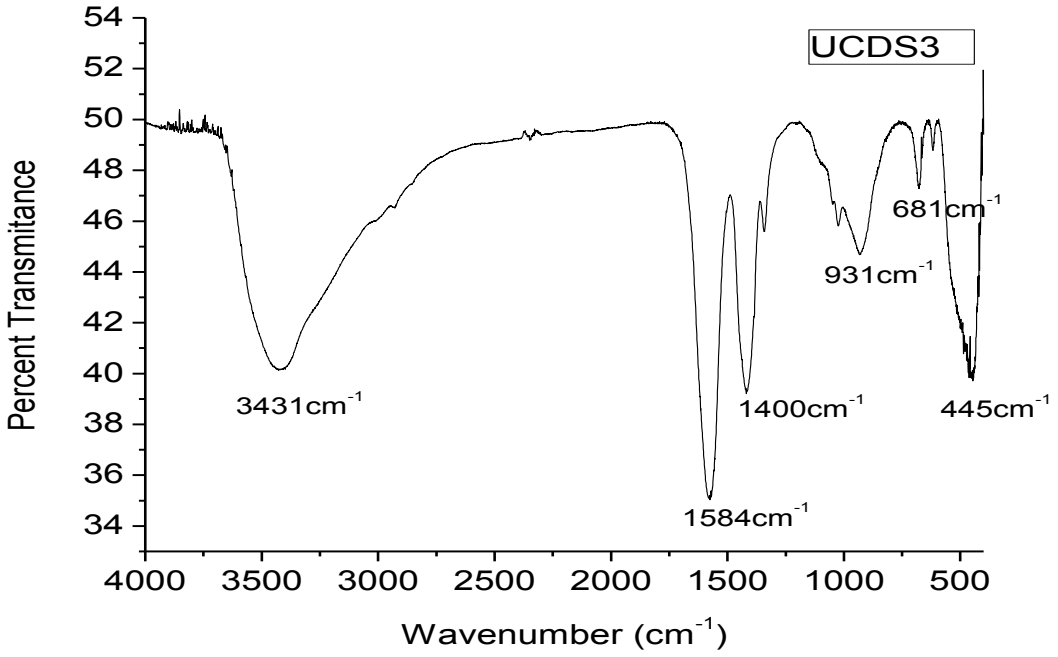

Figure 19: FT-IR spectrum for uncalcinated Cu doped ZnO NPs ($Zn_{1-x}Cu_xO$, x=0.015)

Figure 19 shows the FT-IR spectra of the green synthesized Cu doped ZnO NPs using zinc acetate and copper nitrate before calcinations at temperature of 400 ^{0}C. In the spectrum, the wide absorption band around 3431 cm^{-1} is due to O-H stretching vibrations. The peak around 1584 cm^{-1} could be attributed to the C=O stretching or asymmetric stretching vibration of –COOH, and that around 1400 cm^{-1} corresponded to the (in-plane) bending vibrations of –OH in phenols or symmetric stretching vibration of –COOH functional group. On the other hand, the peak around 931 cm^{-1} represented the presence of C–O-H bending frequency. FT-IR of these peaks suggested the presence of organic components from the neem leaf extract. As it can be seen in Figure 19, for the pure sample, the intense absorption peak at 445 cm^{-1} is related to the

stretching vibrations of Zn–O bond. In the sample doped with copper, an absorption band near 681 cm^{-1} is also recognizable, which is related to vibration of Cu–O bond (Sahar M.D.R, 2006).

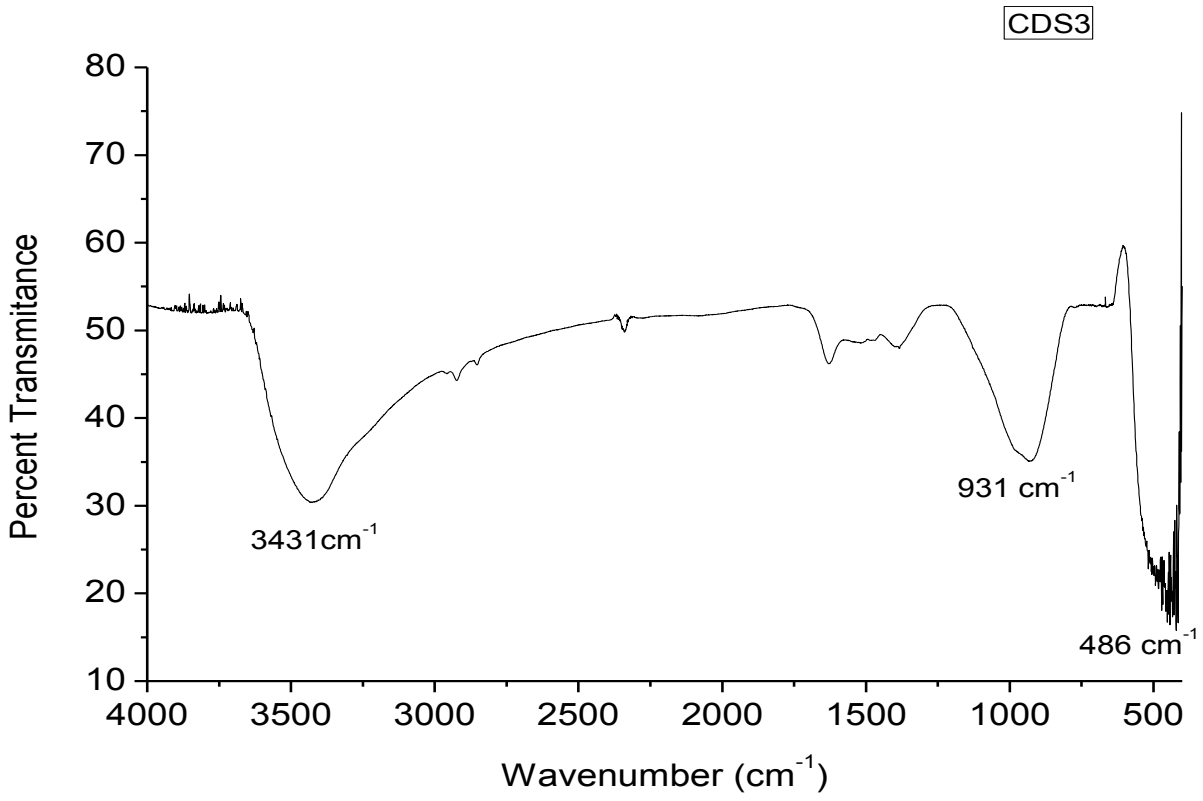

Figure 20: FT-IR spectrum for calcinated Cu doped ZnO NPs ($Zn_{1-x}Cu_xO$, x=0.015)

Figure 20 Shows the FT-IR spectra of the green synthesized Cu doped ZnO NPs using zinc acetate and copper nitrate after calcinations of a temperature at 400 ^{0}C for 1 hr. In the spectrum, the wide absorption band around 3431 cm^{-1} is due to O-H stretching vibrations which has been attributed to –OH group of H_2O, which indicates the existence of water adsorbed on the surface of nanocrystalline powder. The peak around 931 cm^{-1} represented the presence of C–O-H bending frequency. As it can be seen in Figure 20, for the pure sample, the intense absorption peak at 486 cm^{-1} is related to the stretching vibrations of Zn–O bond and the weak peak intensity at 681 cm^{-1} is due to Cu – O bond stretching.-

4.6. UV – Visible Spectroscopy Analysis

The UV-Vis spectra of uncalcined ZnO NP prepared by using zinc acetate (9:1) were shown in Figure 21. The absorption peak of the as-prepared nano ZnO was found at around 368 nm and its sharp absorption feature indicates that the ZnO NPs are monodispersed in nature. The excitonic absorption peak observed due to zinc oxide nanoparticles lies much below the band gap wavelength of bulk zinc oxide 388 nm (Singh, 2009).

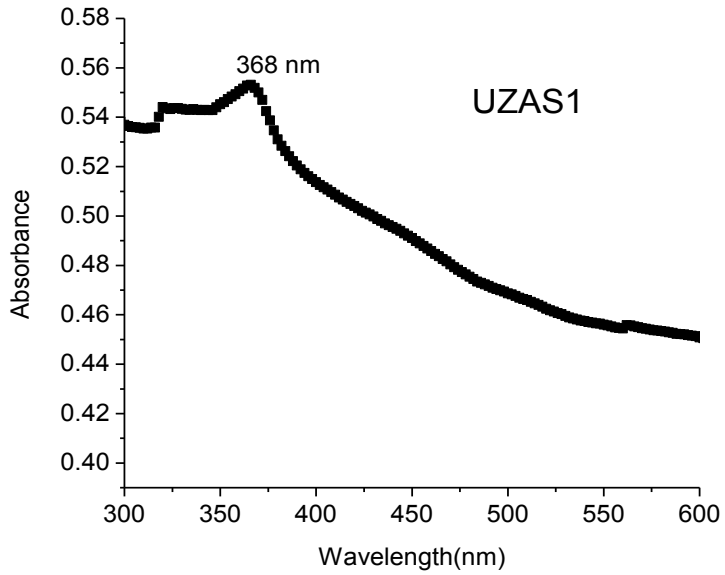

Figure 21: UV-Vis absorbance of uncalcined ZnO NPs synthesized using zinc acetate and Neem leaf extract (9:1).

The UV-Vis absorption spectra of calcined ZnO NP using zinc acetate (9:1) were shown in Figure 22. Absorption spectra of ZnO nanoparticles formed in the reaction media has absorbance maxima at 386 nm. A remarkable broadening of peak indicates that the particles are polydispersed.

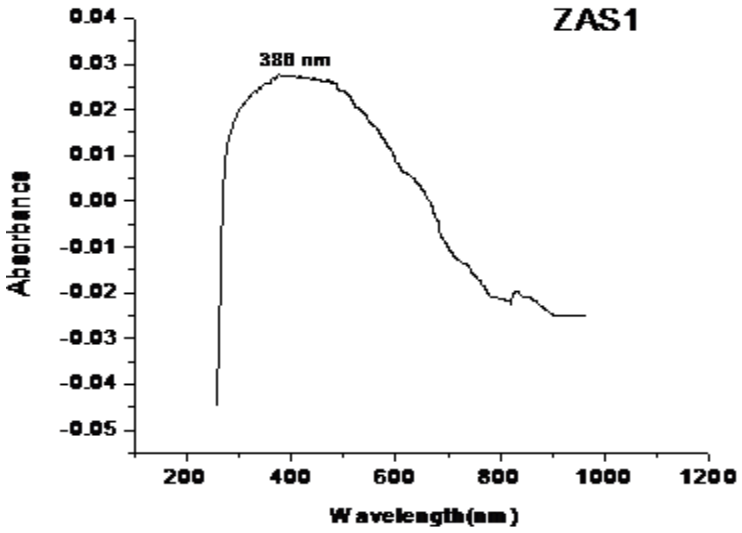

Figure 22: UV-Vis absorbance of calcined ZnO NPs synthesized using zinc acetate and Neem leaf extract (9:1)

As we observe from Figure 22 the absorption peak of the ZnO nanoparticle is broader than the peaks observed in uncalcined ZnO nanoparticles in Figure 21. This indicates that there is a strong interaction between the leaf extract or capping agents and ZnO particles as it confirmed from FT-IR analysis in section 4.5. This might be because of secondary metabolites, alkaloids and flavonoids in the leaf extract (Subramanian SS, 2008).

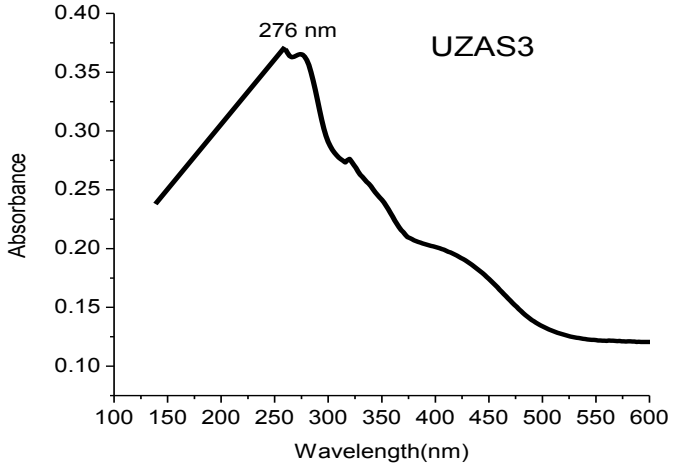

Figure 23: UV-Vis absorbance of uncalcined ZnO NPs synthesized using zinc acetate and Neem leaf extract (7:3)

Figure 23 shows the UV visible spectra of uncalcined ZnO NPs sample using zinc acetate (7:3). The peak absorption spectrum of ZnO NPs for the sample is 276 nm and its sharp absorption feature indicates that the ZnO NPs are monodispersed in nature (Singhal et al., 2011).

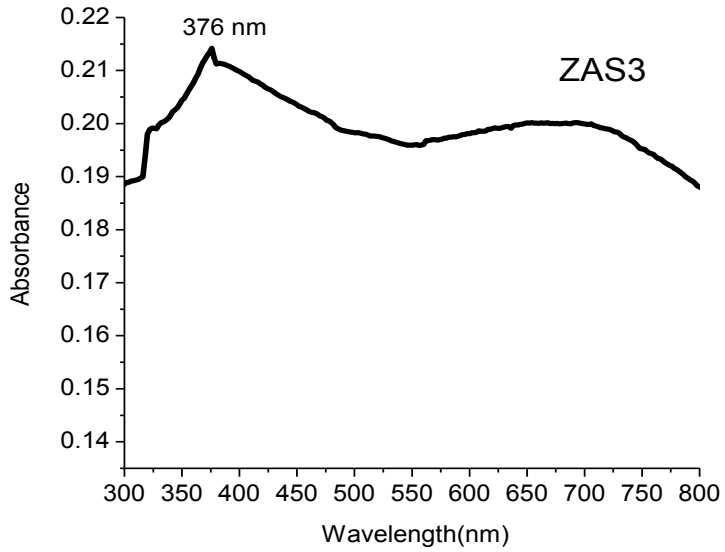

Figure 24: UV-Vis absorbance of calcined ZnO NPs synthesized using zinc acetate and Neem leaf extract (7:3)

Figure 24 shows the UV visible spectra of calcined ZnO NPs sample using zinc acetate (7:3). It depicts the absorption spectrum of the green synthesized ZnO NPs with the absorption peak around 376 nm. The wavelength of 376 nm absorption peak confirms the occurrence of blue-shifted absorption spectrum with respect to the bulk value (388 nm) of the ZnO NPs, due to the quantum confinement effect, which is good agreement of the previous report (Elumalai, 2015).
The spectrum shows the characteristic absorbance peak of ZnO nanoparticles, which confirmed the presence of ZnO nanoparticles.

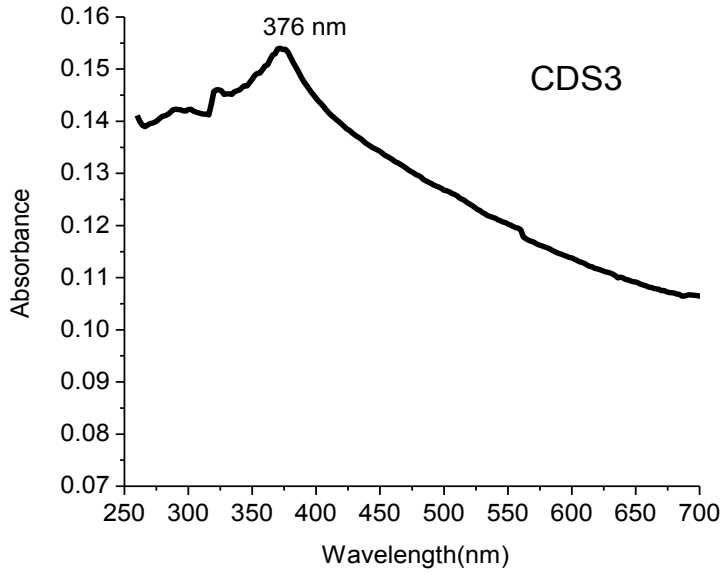

Figure 25: UV-Vis absorbance of calcined Cu doped ZnO NPs ($Zn_{0.985}Cu_{0.015}O$)

Figure 25 shows the UV visible spectra of calcined Cu doped ZnO NPs ($Zn_{0.985}Cu_{0.015}O$). The peak absorption spectrum of doped ZnO NPs for the sample is 376 nm and its sharp absorption feature indicates that the ZnO NPs are monodispersed in nature. The spectrum showed the absorbance peak at 376 nm corresponding to the characteristic band of zinc oxide nanoparticles (Imitan, 2009).

The results for UV- Vis absorption spectrum for calcined ZnO (7:3) and Cu doped ZnO shows that both absorb at 376 nm confirms that zinc oxide nanoparticles were synthesized successfully but for uncalcined ZnO (7:3) lower absorption peak observed at 276 nm due to as-synthesized materials that result from leaf extracts.

4.7. Antibacterial Activity of ZnO NPs and Cu Doped ZnO NPs

The aim of the present study is to determine the antibacterial activity of ZnO nanoparticles and Cu doped ZnO nanoparticles against Gram-positive and Gram-negative bacteria. *Staphylococcus aureus* (*S.aureus*), *Bacillus subtilis*, *Escherichia coli* (*E. coli*) and *Proteus mirabilis* were used as test microorganisms. The antibacterial activity performance of ZnO nanoparticles was done by using disc diffusion method. The effects of particle size and concentration on the antibacterial activity of ZnO nanoparticles were studied using this method. These tests were performed in

nutrient broth and nutrient agar following standard methods. This method is well documented and standard zones of inhibition have been determined for susceptible and resistant values. The zone of inhibition increases with the increase in zinc oxide nanoparticle concentration and decrease in particle size.

In Table 10 zone of inhibition (mm) of the tested samples of ZnO NPs and Cu doped ZnO NPs against four different bacterial strains were given.

Table 10: Zone of inhibition (mm) of ZnO NPs and Cu doped ZnO NPs against gram positive and gram negative bacterial strains

Samples	Zone of inhibition(mm)(Diameter)			
	Gram positive bacteria		Gram negative bacteria	
	Staphylococcus aureus	*Bacillus subtilis*	*Escherichia coli*	*Proteus mirabilis*
ZNS1	9 mm	7 mm	7 mm	6 mm
ZAS1(9:1)	10 mm	6 mm	7 mm	6 mm
ZAS2(7:3)	15 mm	6 mm	6 mm	6 mm
ZAS3(3:2)	12 mm	6 mm	6 mm	6 mm
ZAS4(1:1)	13 mm	6 mm	6 mm	6 mm
CDS1	10 mm	7 mm	6 mm	6 mm
CDS2	8 mm	7 mm	7 mm	6 mm
CDS3	7 mm	8 mm	8 mm	6 mm
UZAS3(7:3)	6 mm	15 mm	6 mm	6 mm
UCDS3 (x=0.015)	6 mm	16 mm	6 mm	6 mm

According to Table 10 ZnO NPs using zinc nitrate are sensitive to gram positive bacteria (*Staphylococcus aureus* and *Bacillus subtilis*) and gram negative bacteria (*E. coli*) but they are resistant to *Proteus mirabilis*. The results showed that ZnO nanoparticles have antibacterial inhibition zone of 9 and 7 mm at the concentration of 10 mg/mL against *S. aureus* and *Bacillus*

subtilis, respectively. This indicates that ZnO NPs are more sensitive to gram positive bacteria. ZnO NPs using zinc acetate are sensitive to *S.aureus* but resistant to *Bacillus subtilis*. They are sensitive to *E. coli* but resistant to *Proteus mirabilis*. In Cu doped ZnO NPs (x=0.005(CDS1), 0.01(CDS2) and 0.015(CDS3)) all are sensitive to gram positive bacteria (*S.aureus* and *Bacillus subtilis*) and gram negative bacteria (*E.coli*). But for x=0.005 sample it is resistant to *E.coli*. All the Cu doped samples are resistant to *Proteus mirabilis*. Zone of inhibition for Cu doped ZnO NPs increases from $Zn_{0.995}Cu_{0.005}O$ to $Zn_{0.985}Cu_{0.015}O$ (6mm to 8mm) on *Bacillus subtilis* and decreases on *S.aureus* (from 10 mm to 7 mm).

From the above results ZnO NPs using zinc nitrate have smaller particle size than zinc acetate so they show greater antibacterial effect than zinc acetate. Similarly, Cu doped ZnO NPs (x=0.015) have showed greater zone of inhibition indicating that they have greater antibacterial effect on gram positive bacteria and gram negative bacteria(*E.coli*) but resistant to *Proteus mirabilis*.

Gram-negative bacteria seemed to be more resistant to ZnO nanoparticles than Gram-positive bacteria. It was found that the antibacterial activity of ZnO nanoparticles increased with decreasing particle size and increasing powder concentration. Their anti-bacterial activity was found higher than reference antibiotic topical dosage forms.

In Table 10 zone of inhibition (mm) of the tested samples of ZnO NPs using zinc acetate and neem leaf extract at different ratios and uncalcined ZnO using zinc acetate(7:3) and uncalcined Cu doped ZnO NPs (x=0.015) against four different bacterial strains were also given.

According to Table 10 ZnO NPs using zinc acetate at 9:1 ratio is resistant to both gram positive and gram negative bacterial strains. ZnO NPs using zinc acetate at 7:3 has greatest zone of inhibition(15 mm) indicating that it has greatest antibacterial activity against *S.aureus*(gram positive bacteria) but it is resistant to *Bacillus subtilis*(gram positive bacteria) and gram negative bacteria(*E.coli* and *Proteus mirabilis*). ZnO NPs using zinc acetate at 3:2 and 1:1 ratios have zone of inhibition 12 and 13 mm respectively on *S.aureus*. This indicates that they have strong antibacterial activity against gram positive bacteria (*S.aureus*). But they are resistant to *Bacillus subtilis* and gram negative bacteria (*E.coli* and *Proteus mirabilis*). From this result gram negative

bacteria are more resistant than gram positive bacteria. So, ZnO NPs synthesized using zinc acetate and neem leaf extract are more effective against *S.aureus.* As the amount of neem leaf extract ratio increases the antibacterial activity of ZnO NPs slightly increases. This could be due to decrease in the size of ZnO NPs with increase in amount of neem leaf extract resulting in high surface area to volume ratio.

On Table 10 uncalcined ZnO NPs using zinc acetate (7:3) has greater zone of inhibition (15mm) than calcined ZnO NPs (7:3) on *Bacillus subtilis*(gram positive bacteria). This indicates that uncalcined ZnO NPs have greater antibacterial effect than calcined one. This is because in uncalcined ZnO NPs there are some bioactive molecules which come from the leaf extract and offer synergistic effects to enhance the antibacterial properties of the synthesized ZnO nanoparticles. However, uncalcined ZnO NPs from zinc acetate are resistant to *S.aureus*(gram positive bacteria) and gram negative bacteria(*E.coli* and *Proteus mirabilis*). Thus, gram negative bacteria are more resistant to the synthesized ZnO NPs which are not calcined than *Bacillus subtilis* (gram positive bacteria). Similarly, uncalcined Cu doped ZnO NPs(x=0.015) have greater zone of inhibition (16 mm) than calcined one (8 mm) on *Bacillus subtilis*. This showed that uncalcined Cu doped ZnO NPs have greatest antibacterial effect on *Bacillus subtilis*. This is due to the presence of some bioactive compounds originated from the leaf extract during ZnO NPs formation in uncalcined ZnO NPs give synergistic effect to enhance the antibacterial properties of the synthesized ZnO NPs.

Table 11: Inhibition zone (mm) size against *Staphylococcus aureus*, *Bacillus subtilis*, and *Escherichia coli* by various antibiotics

Organisms	Antibiotics	ZnO NP and antibiotic	Only antibiotic	Only ZnO NP Samples							
				ZNS 1	ZAS 1	ZAS 2	ZAS 3	ZAS 4	CDS1	CDS2	CDS3
Staphylococcus Aureus	Gentamicin	24	20	9	10	15	12	13	10	8	7
	Ciprofloxacin	20	11	9	10	15	12	13	10	8	7
	Erythromycin	-	-	9	10	15	12	13	10	8	7
Bacillus subtilis	Gentamicin	23	21	7	6	6	6	6	7	7	8
	Ciprofloxacin	20	11	7	6	6	6	6	7	7	8
	Erythromycin	-	-	7	6	6	6	6	7	7	8
Escherichia Coli	Gentamicin	17	16	7	7	6	6	6	6	7	8
	Ciprofloxacin	9	8	7	7	6	6	6	6	7	8
	Erythromycin	-	-	7	7	6	6	6	6	7	8

In Table 11 disc diffusion method was used for the assessment of antibacterial activity. Antibacterial activity of ZnO NPs against *Staphylococcus aureus*, *Bacillus subtilis* and *Escherichia coli* are shown on the basis of the inhibition zone (mm) size in the table. Here the Zone of inhibition is more for both ZnO NPs and antibiotics like gentamycine and ciprofloxacin. Erythromycin has no zone of inhibition as *Staphylococcus aureus*, *Bacillus subtilis* and *Escherichia coli* are not susceptible to Erythromycin.

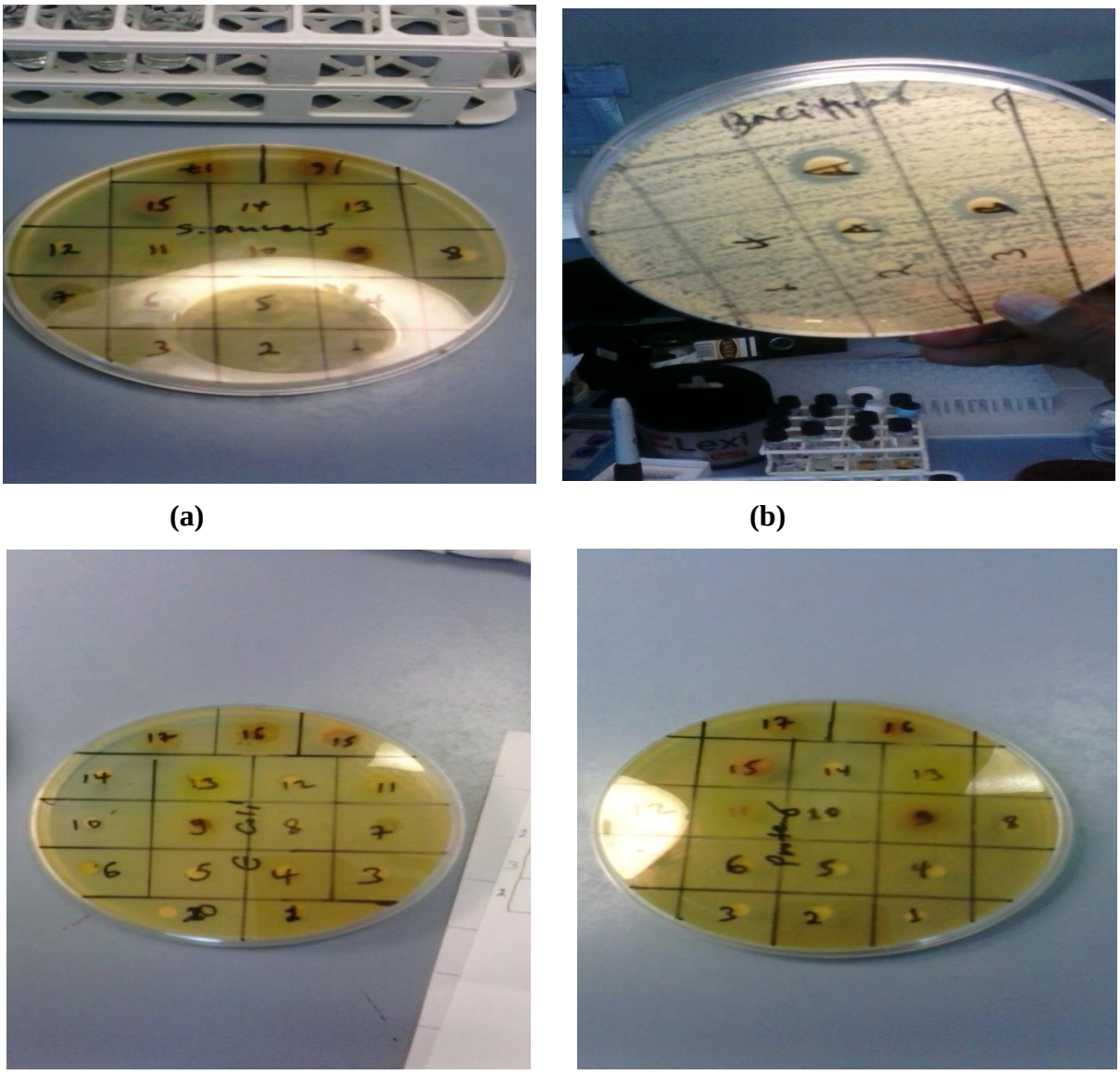

(a) **(b)**

(c) **(d)**

Figure 26: Zone of inhibition of ZnO nanoparticles against (a) *Staphylococcus aureus*, (b) *Bacillus subtilis*, (c) *Escherichia coli* and (d) *Proteus mirabilis*

Figure 26 shows the antibiotic discs in which the antibacterial activity of pure and Cu doped ZnO nanoparticles were tested in Oromiya Public Health Research Laboratory, Adama.

5. CONCLUSIONS

The main objective of the study was to synthesize pure and Cu doped ZnO nanoparticles using leaf extract of *Azadirachta indica* and to study their antibacterial activity against drug resistant bacteria. ZnO NPs and Cu-doped ZnO NPs were successfully synthesized by the biological synthesis method using aqueous leaf extracts and characterized by advanced techniques.

The XRD study confirms the formation of hexagonal wurtzite structure and the crystallite size (16 – 24 nm) of the synthesized ZnO and Cu doped ZnO nanoparticles while the vibrational stretching around 415 cm^{-1} (Zn-O), 625 cm^{-1}(Cu-O) and the characteristic absorption peak observed at 376 nm were also supports the formation of ZnO nanoparticles. The SEM image analyses revealed that the ratio of the leave extract and zinc acetate affects the grain size of synthesized zinc oxide nanoparticles. The EDX studies also confirmed the composition of the synthesized nanoparticles were Zinc and oxygen.

The synthesized ZnO with (9:1) ratio and 1.5% Cu doped ZnO nanoparticles showed significant antibacterial activity against Gram positive and Gram negative bacteria, including *Staphylococcus aureus, Bacillus subtilis,* and *Escherichia coli*. All the synthesized nanoparticles have not sensitive to *Proteus mirabilis* since this bacterium has greatest resistance towards drugs. ZnO nanoparticles have significantly higher antibacterial effect on *S. aureus* indicating that the synthesized ZnO NPs are more sensitive to gram positive bacteria. Compared with Gram-positive bacteria, Gram-negative bacteria are most resistant against antibodies because of their impenetrable cell wall. Consequently, we can propose that ZnO and Cu-doped ZnO NPs at low dopant concentration that can be prepared under the same conditions can be used as an ingredient for the dermatological applications in lotions, creams, ointments, or other biomedical applications. From the result obtained it suggested that the green synthesis is a better choice due to eco-friendliness.

REFERENCES

A. Becheri, M. D. (2008). Synthesis and characterization of zinc oxide nanoparticles:application to textiles as UV-absorbers. *Journal of Nanoparticles Res 10* , 679 - 689.

Aneesh, P. M. (2007). Synthesis of ZnO nanoparticles by hydrothermal method. *Proc. of SPIE 6639* , 66390J - 1.

Ashe, B. (2011). A Detail investigation to observe the effect of zinc oxide and silver nanoparticles in biological system. *Department of Biotechnology & Medical Engineering, National Institute of Technology,Rourkela, India* , 2.

Asmita J.Gavhane., P. P. (2012). Synthesis of silver nanoparticles using extract of neem leaf and triphala and evaluation of their Antimicrobial activities. *Inter.J.Pharma.Bio Sci.* , 0975 - 6299.

Awwad, A. M. (2014). Green synthesis, characterization and optical properties of zinc oxide nanosheets using Olea europea leaf extract. *Adv. Mat. Lett. 5(9)* , 520 - 524.

B. Srinivasa. Reddy, V. K. (2012). *J. Chem. Pharm. Res.* , 4682 - 4694.

Bahttacharjee, C. R.(2011). Homogeneous Chemical Precipitation Route to ZnO Nanospherical. *ISSN 7* , 122 - 127.

Bhattacharya R, M. P. (2008). Biological properties of "naked" metal nanoparticles. *Adv. Drug. Deliv. Rev., View Article Google Scholar 60* , 1289 - 1306.

Bhumkar DR, J. H. (2007). Chitosan reduced gold nanoparticles as novel carriers for transmucosal delivery of insulin. *Pharm Res, View Article Google Scholar 24* , 1415 - 1426.

Brayner, R. e. (2006). Toxicological impact studies based on Escherichia coli bacteria in ultrafine ZnO nanoparticles colloidal medium. *Nano Lett, 6* , 866 - 870.

C. Chen, B. Y. (2007). Investigation of nano - sized ZnO Nanoparticles. *Mater. Lett. 61* , 2961 - 2964.

Callegari A, T. D. (2003). Photochemically grown silver nanoparticles with wavelength - controlled size and shape. *Nano Lett, View Article Google Scholar 3* , 1565 - 1568.

Chehrazi, Z. E.-k. (2011). Antibacterial activity of ZnO nanoparticle on gram positive and gram-negative bacteria. *African Journal of Microbiology Research vol.5(12)* , 1368 - 1373.

Dai J, B. M. (2002). Catalytic nanoparticles formed by reduction of metal ions in multilayered polyelectrolyte films, Nano Lett. *View Article Google Scholar 2* , 497 -501.

Daneshvar, N. A. (2008). Preparation and investigation of photocatalytic properties of ZnO nanocrystals: effect of operational parameters and kinetic study. *Int. J. Chem. Biom. Eng. 1(1)* , 24 - 29.

Dijiken A.V., E. M. (2000). *90* , 123 - 128.

Dimitrijevic NM, B. D. (2001). Radiolytically induced formation and optical absorption spectra of colloidal silver nanoparticles in supercritical ethane. *J Phys Chem B, View Article Google Scholar* , 954 - 959.

Elumalai, K. (2015). Green synthesis of zinc oxide nanoparticles using Moringa oleifera leaf extract and evaluation of its antimicrobial activity. *Spectrochimica Acta Part A: Molecular and Biomolecular Spectroscopy 143* , 158 - 164.

Firouzabadi, M. M. (2015). Antibacterial activity of zinc oxide nanoparticle suspensions on food-borne pathogens. *International Journal Dairy Technology* , 1471 - 0307.

Gayen R.N., D. S., & A.K., P. (2008). *Journal of Crystal Growth, 310* , 4073 - 4075.

Gratzel. (2001). Photo electrochemical cells. Nature. *View Article Google Scholar 414* , 338 - 344.

H. Zhang, B. C. (2011). A strategy for ZnO nanorod mediated multi - mode cancer treatment. *Biomaterials, 32(7)* , 1906 - 1914.

Haritha Meruvu, M. V. (2011). Synthesis and characterization of zinc oxide nanoparticles and its antimicrobial activity against Bacillus subtilis and Escherichia coli. *RASAYAN J. Chem.vol.4, No.1* , 0974 - 1496.

Imitan, S. A. (2009). Solvothermal Synthesis and Properties Control of Doped ZnO Nanoparticles. *Journal of Colloid and Interface Science, 329* , 73 - 80.

Iravani, S. (2011). Green Chemistry. *13* , 2638 - 2650.

J Yu, M. B. (2011). Effects of physiochemical properties of zinc oxide nanoparticles on cellular uptake. *Journal of Physics: Conference Series 304* , 012 - 044.

J.T. Seil, E. T. (2009). Reduced activity of Staphylococcus epidermidis in the presence of sonicated piezoelectric zinc oxide nanoparticles. *IEEE 35th Annual Northest Bioengineering Conference* , 1 - 2.

Jana, N. a. (2000). Seed-mediated growth method to prepare cubic copper Nanoparticles. *Current Science 79(9)* , 1367 - 1370.

L. Zhang, Y. J. (2007). Nanoparticles. *Res.9* , 479 - 489.

M. Moritz, M. G. (2013). *Chem. Eng. J.;228* , 596 - 613.

M. Premanathan, K. K. (2011). Nanomed. *Nanotech. Biol. Med.7* , 184 - 192.

Manokari M, R. C. (2016). Biosynthesis of Zinc oxide NPs using Melia azedarach L. extracts and their Characterization. *Biotechnology Laboratory, Department of Plant Science. M.G.G.A.C, Mahe, Pondicherry, India* , 31 - 36.

Monica, N. N. (2013). Synthesis of Silver Nanoparticles using Azadirachta indica (Neem) extract and usage in water purification. *Asian J.Pharm.Tech;vol3* , 170 - 171.

Murray CB, S. S. (2001). Monodisperse 3d transition-metal(Co, Ni, Fe) nanoparticles. *MRS Bull, View Article Google Scholar 26* , 985 - 991.

N. Rajagopalan, A. K. (2013). Effect of nano ZnO in lowering yellowing of aliphatic amine-cured DGEBA based epoxy coatings on UV exposure. *IJARPS* , 7 -12.

N. Srinivasa Rao, M. B. (2015). Structural and optical investigation of ZnO nano powders synthesized from zinc chloride and zinc nitrate. *American Journal of Materials Science 5(3)* , 66 - 68.

Nagajyoti, P. P. (2011). Biofabrication of silver nanoparticles using leaf extract of Saururus chinenis. *Digest J.Nanomat. Biostruct.* , 121 - 133.

Okuda M, K. Y. (2005). Self-organized inorganic nanoparticle arrays on protein lattices. *Nano Lett. View Article Google Scholar 5* , 991 - 993.

Padmavathy, N. a. (2008). Enhanced bioactivity of ZnO nanoparticles -an antimicrobial study. *Sci. Technol. Adv. Mater,9* , 1 - 7.

Pesika NS, Stebe KJ, Searson PC (2003). Determination of the particle size distribution of quantum nanocrystals from absorbance spectra. *Adv. Matter., 15*: 1289-1291

Rai, M. e. (2008). A Current trends in phytosynthesis of metal nanoparticles. *Critical Reviews in Biotechnology 28(4)* , 277 - 284.

Ramani, M. P. (2012). Zinc oxide nanoparticles: A study of defect level blue-green emission. *Optical Materials 34* , 817 - 820.

Reddy, V. (2006). Gold nanoparticles: Synthesis and applications. *Synlett,11* , 1791 - 1792.

S. Baruah, S. S. (2009). *J. Appl. Phys. 105* , 743 - 748 .

Singh, A., Viswanath, V. & Janu, V. (2009). Synthesis, effect of capping agents, structural, optical and photoluminescence properties of ZnO nanoparticles. *J. Lumin.*, 129(8), 874–878.

S. Jurablu, M. F. (2015). Sol-gel synthesis of zinc oxide (ZnO) nanoparticles: Study of Structural and Optical Properties. *Journal of Sciences, Islamic Republic of Iran 26(3)* , 281 - 285.

S. Kuriakose, N. e. (2013). Nanotechnology. *4* , 763 - 770.

S.P. Chandran, M. C. (2000). *22* , 577 - 583.

S.S. Kulkarni, M. S. (2015). Optical and structural properties of zinc oxide nanoparticles. *International Journal of Advanced Research in Physical Science(IJARPS), 2(1)* , 14 - 18.

Sahar M.D.R, B. A. (2006). *Journal of Solid state Science and Technology,14* , 115-116.

Sathya, A. a. (2012). Studies on the phytochemistry, Antimicrobial activity and green synthesis of nanoparticles using Cassiatora L. *Drug invent.* , 408 - 410.

Senthilkumar, S. a. (2014). Green Tea (Camellia sinensis) mediated synthesis of Zinc oxide (ZnO) nanoparticles and studies on their Antimicrobial activities. *International Journal of P*

Singhal et al. (2011). Biosynthesis of ZnO nanoparticles using *Ocimum sanctum* (Tulsi) leaf extract and screening its antimicrobial activity. *Journal of Nanoparticle Research, 13*, 2981-2988.

Slman, A. A. (2012). Antibacterial activity of ZnO nanoparticle on some gram-positive and gram-negative bacteria. *Iraqi Journal of physics,vol.10, No. 18* , 5 - 10.

Snehal Yedurkar, C. M. (2016). Biosynthesis of Zinc Oxide NPs Using Ixora Coccinea Leaf Extract - A Green Approach. *Open Journal of Synthesis Theory and Applications,5* , 1 - 14.

Subramanian SS, N. S. (2008). Phytochemical studies on Azadirachta indica. *Planta Medica;16* , 432 - 435.

Sun Y, Y. Y. (2002). Uniform form silver nanowires synthesis by reducing AgNO3 with ethylene glycol in presence of seeds and poly(vinyl pyrrolidone). *Chem Mater 14* , 4736 - 4745.

Tamanna Bhuyan, K. M. (2015). Biosynthesis of zinc oxide nanoparticles from Azadirachta indica for antibacterial and photocatalytic applications. *Materials science in semiconductor processing 32* , 55 - 61.

Theodore, L. (2006). Nanotechnology: Basic calculations for Engineers and Scientists. *Wiley, Hoboken* , 345 - 349.

Wang, L. M. (1999). Synthesis of zinc oxide nanoparticles with controlled morphology. *J. Mater. Chem.9* , 2871 - 2878.

Wildenberg, V. d. (2005). Roadmap report on nanoparticles. *View Article Google Scholar W & W Espana sl, Barcelona, Spain* , 256 - 260.

Willner B., B. B. (2007). Nanoparticle-enzyme hybrid system for nanotechnology. *FEBS Journal 274* , 302 - 309.

Yamada, H. e. (2007). Gene Expression Profile in Human Cells Exposed to Zinc. *J. Toxi. Sci.32,* 193 - 196.

Yamamoto, O. -S. (2000). Change in Antibacterial Characteristics with Doping Amount of ZnO in MgO - ZnO Solid Solution. *International Journal of Inorganic Materials, 2,* 451 - 454.

Yin B, M. H. (2003). Electrochemical synthesis of silver nanoparticles under protection of poly (N-Vinylpyrrolidone). *J Phys Chem B, View Article Google Scholar 107,* 8898 - 8904.

Z.Y. Fan, J. L. (2005). Zinc oxide nanostructures synthesis and properties. *Journal of Nanoscience and nanotechnology 5* , 1561 - 1567.

Zhang L, S. Y. (2006). One - step synthesis of monodisperse silver nanoparticles beneath vitamin E Langmuir monolayers. *J Phys Chem B, View Article Google Scholar,110,* 6615 - 6620.

ZL, Wang. (2004). Zinc oxide nanostructures: growth, properties and applications. *J Phys Condens Matter* , 829 - 858.

APPENDICES

Appendix 1: XRD pattern for ZnO NPs using Zinc nitrate precursor

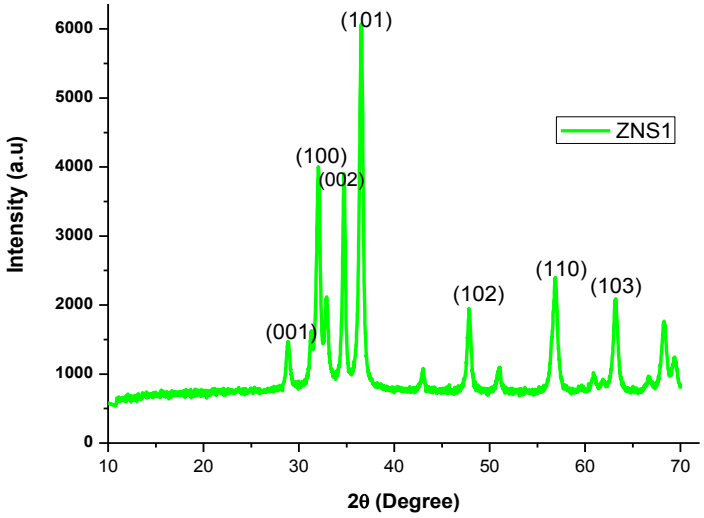

Appendix 2: XRD pattern for ZnO NPs using Zinc acetate precursor

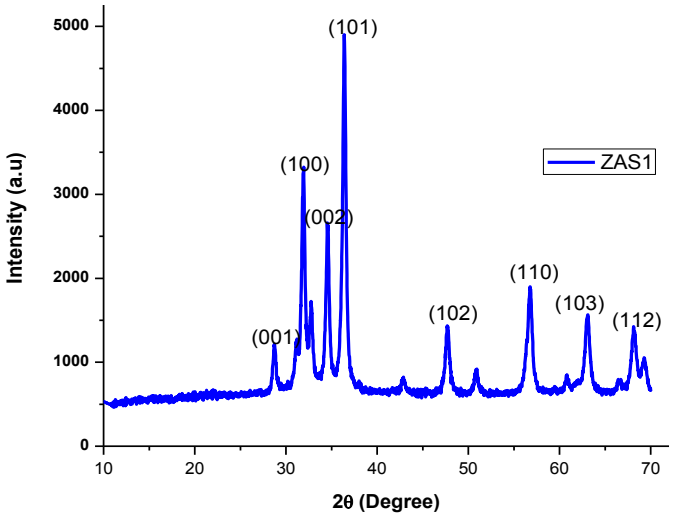

Appendix 3: XRD pattern for Cu doped ZnO NPs ($Zn_{0.995}Cu_{0.005}O$)

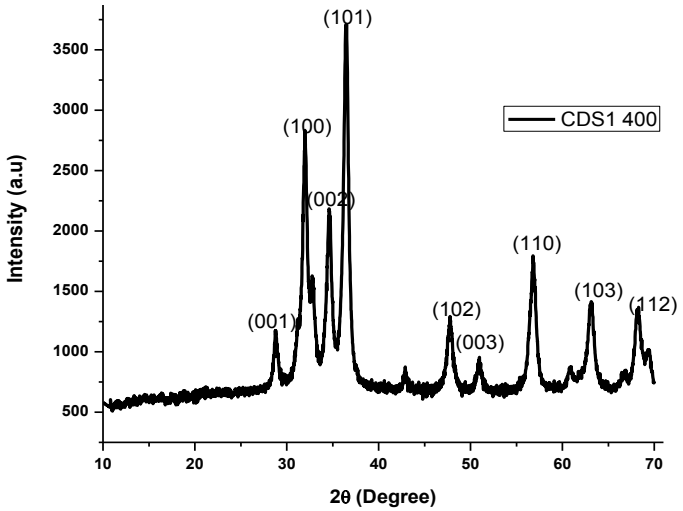

Appendix 4: XRD pattern for Cu doped ZnO NPs ($Zn_{0.985}Cu_{0.015}O$)